Two Dimensional Mathematical Model of Evacuated Tubular Solar Collector

by

Faizur-Rahman

A Thesis Presented to the

FACULTY OF THE COLLEGE OF GRADUATE STUDIES

KING FAHD UNIVERSITY OF PETROLEUM & MINERALS

DHAHRAN, SAUDI ARABIA

In Partial Fulfillment of the
Requirements for the Degree of

MASTER OF SCIENCE

In

CHEMICAL ENGIEERING

February, 1981

INFORMATION TO USERS

This manuscript has been reproduced from the microfilm master. UMI films the text directly from the original or copy submitted. Thus, some thesis and dissertation copies are in typewriter face, while others may be from any type of computer printer.

The quality of this reproduction is dependent upon the quality of the copy submitted. Broken or indistinct print, colored or poor quality illustrations and photographs, print bleedthrough, substandard margins, and improper alignment can adversely affect reproduction.

In the unlikely event that the author did not send UMI a complete manuscript and there are missing pages, these will be noted. Also, if unauthorized copyright material had to be removed, a note will indicate the deletion.

Oversize materials (e.g., maps, drawings, charts) are reproduced by sectioning the original, beginning at the upper left-hand corner and continuing from left to right in equal sections with small overlaps. Each original is also photographed in one exposure and is included in reduced form at the back of the book.

Photographs included in the original manuscript have been reproduced xerographically in this copy. Higher quality 6" x 9" black and white photographic prints are available for any photographs or illustrations appearing in this copy for an additional charge. Contact UMI directly to order.

Order Number 1355740

Two dimensional mathematical model of evacuated tubular solar
collector

Faizur-Rahman, M.S.

King Fahd University of Petroleum and Minerals (Saudi Arabia), 1981

TWO DIMENSIONAL MATHEMATICAL MODEL OF
EVACUATED TUBULAR SOLAR COLLECTOR

by

FAIZUR-RAHMAN

THESIS

Presented to

THE COLLEGE OF GRADUATE STUDIES

University of Petroleum & Minerals
Dhahran, Saudi Arabia

In Partial Fulfillment of the
Requirements for the Degree of

MASTER OF SCIENCE IN CHEMICAL ENGINEERING

FEBRUARY 1981

UNIVERSITY OF PETROLEUM & MINERALS

DHAHRAN, SAUDI ARABIA

This thesis, written by Faizur-Rahman under the direction of
his Thesis Committee, and approved by all its members, has
been presented to and accepted by the Dean, College of Graduate
Studies, in partial fulfillment of the requirements for the
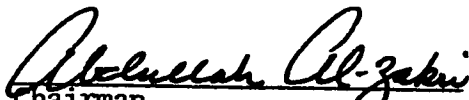degree of MASTER OF SCIENCE IN CHEMICAL ENGINEERING

_____
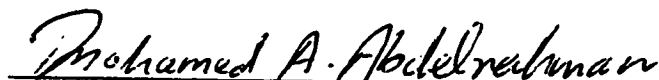Dean, College of Graduate Studies

Date _____

_____
Department Chairman

THESIS COMMITTEE

_____
Chairman

_____
Member

_____
Member

To my mother

and in memory of my father

ACKNOWLEDGEMENTS

A B S T R A C T

Presently available performance models of evacuated
tubular solar collectors uses HWB model to determine
useful energy gain. The main shortcoming of HWB model
is that it is basically one-dimensional and is based on
lumped formulation. The errors associated with using this
model are compounded by the fact that the model is not
conservative but gives results that are too high. A compre-
hensive literature search indicated that evacuated tubular
solar collectors have not yet been analysed considering
two dimensional effects in the absorber plate. It is
believed that the two dimensional analysis will enable a
more accurate evaluation to be made of the collector
performance.

In this thesis parametric analysis of evacuated
tubular solar collector is presented developing two
dimensional performance model. The collector uses a thin
flat plate spanning its diameter as its absorbing surface.
Collectors of this type are being commercially produced
by Corning Glass Works, N.Y.

In the analysis of the plate assuming the temperature
gradient to be negligible along the plate thickness reduces
the problem to a two dimensional one. For the fluid inside
the tube, radial variation of temperature is neglected.

Energy balances are made on collector plate and tube
each considered as a separate unit and two differential
equations are obtained. The solution to the differential
equations gives the temperature distributions of the
plate and fluid. The heat loss model developed allows
for wide flexibility in ambient temperature, collector
temperature, fluid flow rate etc. The model includes
optical effects also.

Two-dimensional temperature distribution has been
illustrated by isotherms. Performance curves obtained from
two-dimensional model has been compared with that of
HWB model. It was found that HWB model over-estimates
performance by less than 1 percent at higher flow rates
and about 3.5 percent at low flow rates. Plate thickness
has negligible effect on collector performance. Increase
in tube spacing or length increases fluid outlet temperature
and decreases efficiency, but it is more efficient to
increase fluid outlet temperature by increasing length
rather than water tube spacing.

TABLE OF CONTENTS

LIST OF FIGURES

ix

LIST OF TABLES

NOMENCLATURE

A_g $D_g L$ - Front surface area of glass tube.

A_p Absorber plate area.

C_p Average fluid specific heat.

C_b Bond conductance.

C_n n^{th} coefficient of the infinite series in the temperature expressions.

D Outside diameter of flow channel.

D_g Outside diameter of glass tube.

D_i Inside diameter of flow channel.

f $=$ $L/R\dot{m}C_p$.

F Standard fin efficiency

F' Collector efficiency factor.

F_R Collector heat removal factor.

g $=$ $(W - D)/4K_p \delta_p R$.

G $=$ $\dot{m}/A_p$.

h $=$ $DU_L(W - D)/4K_p \delta_p$.

$h_{g,r}$ Radiation heat transfer coefficient from the glass tube surface.

$h_{p,r}$ Radiation heat transfer coefficient between the absorber plate and glass tube.

h_w Convection heat transfer coefficient around a cylinder.

h_{wp} Adjusted convection heat transfer coefficient of glass tube surface.

h_f Convection heat transfer coefficient between the coolant fluid and the flow channel.

I Total solar radiation on a tilted surface.

K_p Thermal conductivity of the absorber plate.

L Length of the absorber plate.

$m \;=\; (U_L/K_p \delta_p)^{\frac{1}{2}}$

$\dot{m}$ Mass flow rate through each flow channel.

$P \;=\; (\frac{W - D}{2}) \cdot \frac{1}{L}$

q_u Useful gain introduced in two-dimensional model.

$q_u^{'}$ Useful gain introduced in one-dimensional model.

$q_{fin\text{-}base}^{'}$

Energy conducted to the region of the tube per unit of length in the flow direction.

$q_{tube}^{'}$

Energy collected above the tube region per unit of length in the flow direction.

$$Q^2 = U_L \left(\frac{W - D}{2}\right)^2 / K_p \delta_p$$

Q_L Heat lost by the collector.

Q_u Total useful energy gain of the collector.

$R = \left(\frac{1}{h_f \pi D_i} + \frac{1}{C_b}\right)$

$S = (\tau\alpha) I$

T_a Ambient temperature.

T_b Absorber plate temperature above the bond.

T_f Fluid temperature.

$T_{f,i}$ Fluid inlet temperature.

$T_{f,m}$ Average temperature of the fluid.

$T_{f,o}$ Fluid outlet temperature.

$T_f^* = \dfrac{\theta_f}{\theta_{f,i}}$ - Non-dimensional fluid temperature distribution.

$T_{f,m}^*$ Non-dimensional average temperature of fluid.

T_g Temperature of the glass tube.

T_p Plate temperature.

$T_{p,m}$ Average temperature of the plate.

$T_p^* = \dfrac{\theta_p}{\theta_{f,i}}$ - Non-dimensional plate temperature distribution.

$T_{p,m}^*$ Non-dimensional average plate temperature.

T_s Equivalent sky temperature as a function of the ambient air temperature.

U_L Collector overall loss coefficient.

V Wind speed.

W The distance between the flow channels.

x Transverse dimension normal to the flow channel.

$x^* = x/(\dfrac{W - D}{2})$ - Non-dimensional transverse coordinate.

y Axial dimension parallel to the flow channel.

$y^* = y/L$ - Non-dimensional axial coordinate.

α Absorptivity of the absorber plate.

γ Non-dimensional parameter.

$\gamma_n = (\lambda_n^2 + Q^2)^{\frac{1}{2}}.$

δ_p Absorber plate thickness.

ε_p Absorber emissivity.

ε_g Emissivity of the glass.

ε_{pg} Effective emissivity between the absorber plate and glass.

η Instantaneous collector efficiency.

$\theta_p = T_p - T_a - S/U_L.$

$\theta_f = T_f - T_a - S/U_L.$

λ Arbitrary separation constant.

$\lambda = n\pi P$

$$\lambda_n^* \quad = \quad n\pi$$

$$\xi_n \quad = \quad \lambda_n^*/f$$

ρ Reflectance of glass surface

σ Stefan-Boltzmann Constant

τ $\tau_{r,1} \tau_a$ - Transmittance allowing for both reflection and absorption.

τ_a Transmittance considering only absorbion.

τ_{avg} Average transmittance

$\tau_{r,1}$ Transmittance for a single cover neglecting absorption.

$(\tau\alpha)$ Effective transmittance - absorptance product.

CHAPTER I

INTRODUCTION

Energy is always a very important factor to provide man with enough food and adequate shelter and clothing. As a result of projected world energy shortage the use of solar energy for environmental control is receiving much attention in the engineering sciences literature. The sun is a source of nearly all forms of energy on the earth. Our earth receives a continuous stream of energy from the sun. On a clear day the earth receives IKW of solar energy for each square meter of surface for a few hours per day. Perhaps 4 to 8 KWhr/m² day can be collected.

In a solar installation the solar collector is the essential item, and it is here that solar radiant energy is transformed to some other useful energy form. The facts that solar energy, like carpeting, comes by the square meter and that the first cost of the collector per square meter is appreciable makes solar collectors capital intensive. Significantly large sums of capital must be invested in return for the use of this non-depletable source of energy.

The flat plate collector is the simplest and
one of the cheapest means of collecting solar energy
for use in systems that require thermal energy at low
temperatures (<100°C).

As solar energy is a dispersed form of energy,
an effective method of collection is very important.
It is well-known that by evacuating a solar collector
its performance can be highly improved. Evacuated tube
solar collectors permit the use of a vacuum of sufficient
magnitude (about 10^{-4} mm Hg) to eliminate convection and
conduction heat transfer losses. The vacuum may help
to protect a selective surface used on the absorber (for
reduction of long-wave radiation heat losses) against
performance degradation over the life of the collector.
Also, these collectors permit the collection of solar
energy at lower solar radiation levels i.e. earlier in
the morning and later in the evening. In addition, these
collectors generally require a minimum amount of material
per square meter of collector and thus provide for the
possibility of lower costs.

A typical evacuated collector tube detail is shown
in Figure 1.1. Collectors of this type are being commer-
cially produced by Corning Glass Works[1], New York.
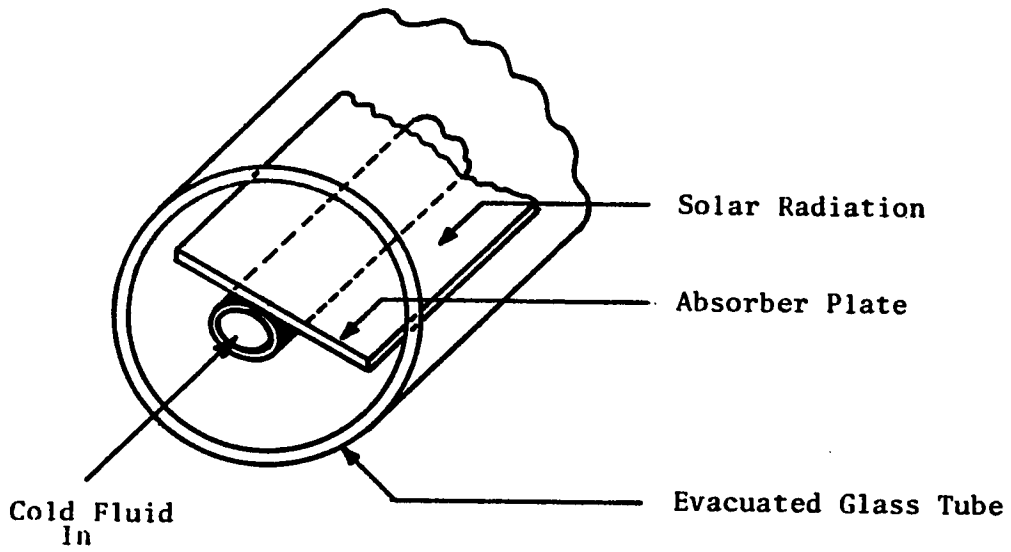
Figure 1.1 : An Evacuated Tubular Solar Collector

In the present study a two dimensional mathematical model is developed for evacuated tubular solar collectors which uses for its absorbing surface a thin flat plate spanning its diameter. The emphasis of the investigation is to study the two dimensional effects in the absorber plate housed in evacuated glass cylinders.

It has been found by Klein et al[2], that a zero capacitence model is quite adequate when hourly meteorological data are used, and hence in this study steady state analysis of the collector is made. The overall loss coefficient has been assumed constant for the whole plate. The effects of various parameters on the temperature distribution and efficiency are studied under different conditions. Since a theoretical analysis is the basis for most competitive designs, mathematical models are necessary for designers of solar collectors to maximize the net collection Vs cost.

CHAPTER II

LITERATURE REVIEW

Recently, a measure of success has been achieved
in producing evacuated collectors by employing a cylindrical
glass envelope, design (1, 3-5). Although evacuated
collectors with a flat plate cover can be constructed,
there are structural advantages with a cylindrical tube
and the construction of a collector is much simpler than
using a flat glass plate. The absorber plate, contained
within this cylinder, may be another glass cylinder,
concentric with the outer one[3], a flat plate[1], or a
single U-tube in which case the rear half of the glass
cylinder is given a reflective coating to form a concentrator,
and the U-tube is placed at the focus[5]. The absorber is
suspended in the envelope with minimum contact area of the
supports with the glass tube.

Karaki et al[6], Hinotani et al[7], Felske[8], and
others developed performance model and analysed evacuated
cylindrical solar collectors. They considered optical
effects and used HWB model to obtain useful energy gain
of the collector. The main short coming of this model is
that it is basically one-dimensional and is based on lumped

formulation. The configuration parameters of the collector
do not appear explicitly in the efficiency expression
but are reflected through various efficiency factors.
The internal resistances of the plate and tube are
neglected. Duffie and Beckman[9] refined the lumped
analysis by taking into account the resistances between
the tube and the fluid, by first obtaining an expression
for the average fluid temperature, and then calculating
the average plate temperature by including a resistance
between the two temperatures.

A review of existing literature indicated that,
although the effects of various collector parameters on
the collector efficiency were well documented based on
extensive experimentation, a rigorous theoretical analysis
is lacking in this area.

The analysis which results in HWB model neglects
axial conduction in both the fluid and the receiver.
Phillips[10] presented a closed form solution which predicts
the performance of a flat plate solar collector including
the effect of axial conduction in the receiver. Since fluids
with high thermal conductivity such as liquid metals, are
not commonly used as collector coolants, the assumption of

negligible axial conduction in the transfer fluid seems reasonable. Collector plates, on the other hand, are often designed to be good conductors in order to efficiently transfer heat from the absorbing surface to the transfer fluid. Thus it does not seem appropriate to neglect axial conduction in the receiver under all conditions. Axial conduction in the collector plate causes a flow of heat in the direction opposite to the flow of fluid. This results in a reduction of the fluid outlet temperature and overall efficiency of the system. The errors associated with using HWB model are compounded by the fact that the model is not conservative but gives results that are too high.

Kirchhoff[11], Chiou[12] and others analysed flat plate solar collector by developing a two-dimensional performance model of flat plate collector.

It appears from previous literature search that evacuated cylindrical solar collectors have not yet been analysed considering two-dimensional effects in the absorber plate. To study the two-dimensional effects in flat plate housed in evacuated glass cylinders the following work has been carried out. It is believed that two-dimensional

analysis will enable a more accurate evaluation to be made of the collector performance.

One-Dimensional Collector Model

Based on the pioneering work of Hottel and Woertz[13] (1942), Hottel and Whillier[14] (1953) developed a one-dimensional model of a flat plate solar collector. Further analytical studies were made by Bliss[15] (1959) using a similar model. Most of the research that is being conducted in solar energy is based on the steady-state models of Hottel, Whillier and Bliss (HWB). Duffie and Beckman have presented HWB model in detail, a brief description of it is given here.

The simplifying assumptions used in the analysis are listed below:

1. Performance is steady-state.

2. Construction is of sheet and tube type.

3. The headers provide uniform flow to tubes.

4. The headers cover a small area of collector and can be neglected.

5)   The overall loss coefficient U_L may be treated
        as independent of position.

6)   The temperature gradient across the absorber plate
        thickness is negligible.

7)   Flow properties may be evaluated at a mean fluid
        temperature.

8)   Shading of the collector absorbing plate is
        negligible.

9)   The tube spacing is constant with the edge tube
        located inward a distance of one-half the spacing.

10)   Axial conduction in the absorber plate does not
        effect the local plate conductance for transverse
        heat flow.

There are more assumptions relating to the
evaluation of U_L which are not given here but can be
found in (9).

Following is the analysis presented by Duffie and
Beckman[9]. The first step in a thermal analysis of the
absorber plate-tube assembly is to obtain expressions for
the temperature distribution in the region between tubes.
Using the previously noted assumptions for parallel-flow

collectors, symmetry can be used to separate the
individual tube-sheet sections by insulated boundary
conditions at locations midway between tubes. Within
each separated section, symmetry again exist for each
half-width region. Figure 2.1 shows one such region,
on which a one-dimensional thin-fin thermal analysis
will be made. Applying an energy balance on the fin
element gives the following differential equation
applicable for $0 \leq x \leq \frac{W-D}{2}$.

$$\frac{d^2 T_p}{dx^2} = \frac{U_L}{K_p \delta_p} (T_p - T_a - S/U_L) \qquad (2.1)$$

The two boundary conditions necessary for this second-
order differential equation are symmetry at the centerline
and known root temperature;

$$\left. \frac{dT_p}{dx} \right|_{x = 0} = 0 \qquad \text{and} \qquad \left. T_p \right|_{x = \frac{W-D}{2}} = T_b$$

where $T_p = T_p (x)$

If we define $m^2 = U_L/K_p \delta_p$ and $\theta_p = (T_p - T_a - S/U_L)$
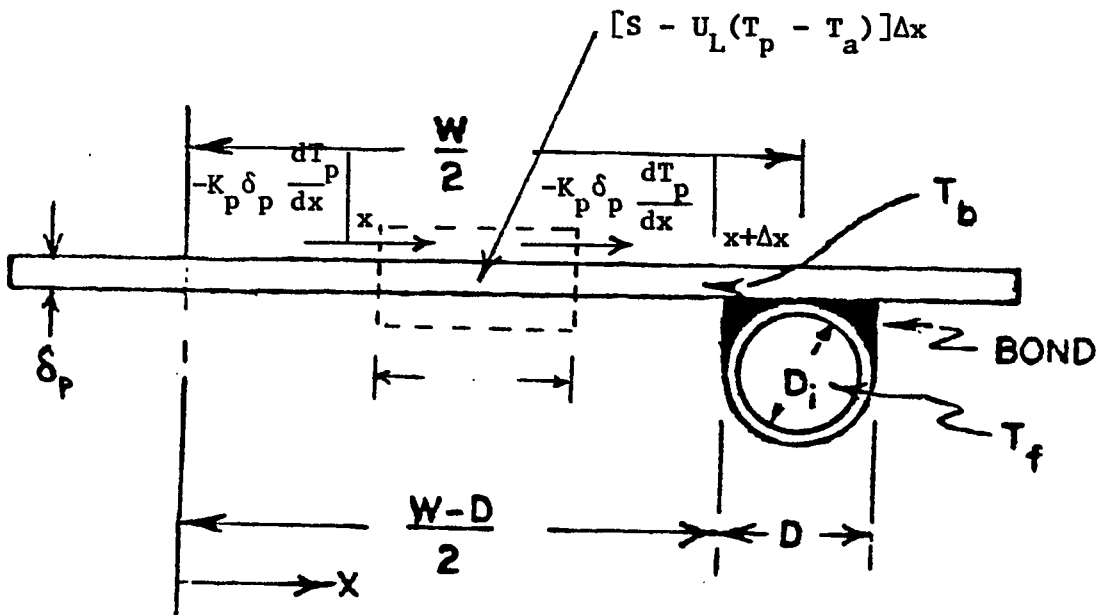
Figure 2.1: Sheet and tube dimensions and energy balance.

The solution to equation (2.1) will be

$$\frac{\theta_p}{\theta_b} = \frac{\text{Cosh } m \ x}{\text{Cosh } m \ (W-D)/2} \qquad (2.2)$$

The energy conducted to the region of the tube per unit of length in the flow direction can now be found by evaluating Fourier's law at the fin base:

$$q'_{fin-base} = -2K_p \delta_p \left. \frac{dT_p}{dx} \right|_{x \ = \ (W-D)/2} \qquad (2.3)$$

where the factor of 2 results from heat flow into both sides of the tube base. Using equation (2.2), equation (2.3) may be written as:

$$q'_{fin-base} = -(W-D) F \ U_L \ A_b \qquad (2.4)$$

where F is the standard fin efficiency given by

$$F = \frac{\tan h\{m(W-D)/2\}}{m(W-D)/2} \qquad (2.5)$$

The useful gain of the collector also includes the energy collected above the tube region. The energy

gain for the tube region is:

$$q'_{tube} = D\{S-U_L(T_b - T_a)\} \qquad (2.6)$$

or in terms of θ_b

$$q'_{tube} = -DU_L\theta_b \qquad (2.7)$$

The total useful gain for the collector per unit of length in the flow direction becomes:

$$q'_u = -\{(W-D)F + D\} U_L\theta_b \qquad (2.8)$$

Ultimately, the useful gain from equation (2.8) must be transferred to the fluid. The resistance to heat flow to the fluid results from the bond and the fluid to tube resistance. The useful gain can be expressed in terms of these two resistances as:

$$q'_u = \frac{(T_b - T_f)}{1/h_f \ \pi D_i + 1/C_b} \qquad (2.9)$$

or $\quad q'_u = \dfrac{\theta_b - \theta_f}{1/h_f \ \pi D_i + 1/C_b} \qquad (2.10)$

where D_i is the inside tube diameter and h_f is the heat transfer coefficient between the fluid and the tube wall. C_b is the bond conductance.

Solving equation (2.10) for θ_b, substituting it into (2.8), and solving the result for the useful gain, we obtain,

$$q_u' = -WU_L F' \theta_f \qquad (2.11)$$

where $\theta_f = (T_f - T_a - S/U_L)$ and F', the collector efficiency factor, is given by:

$$F' = \cfrac{1/U_L}{W\left[\cfrac{1}{U_L [D + (W - D)F]} + \cfrac{1}{C_b} + \cfrac{1}{h_f \pi D_i}\right]} \qquad (2.12)$$

The useful gain per unit of flow length as calcualted from equation (2.11) is ultimately transferred to the fluid. The fluid enters the collector at temperature $T_{f,i}$ and increases in temperature until at exit it is $T_{f,0}$. Referring to Figure 2.2, an energy balance can be made on the fluid flowing through a section of one pipe of length Δy as
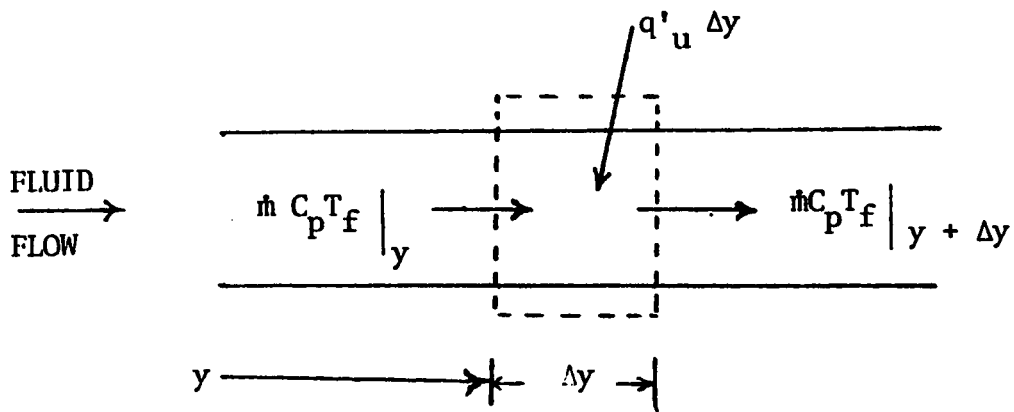
Figure 2.2: Energy balance on Fluid element.

$$\dot{m}C_p \frac{dT_f}{dy} - q_u' = 0 \qquad (2.13)$$

or
$$\dot{m}C_p \frac{d\theta_f}{dy} + WU_L F' \theta_f = 0 \qquad (2.14)$$

Applying boundary condition

$$\theta_f(0) = \theta_{f,i}$$

Equation (2.14) has the solution

$$\frac{\theta_f(y)}{\theta_{f,i}} = \exp(- U_L F' y / \dot{m} C_p) \qquad (2.15)$$

The collector heat removal factor F_R can be obtained from equation (2.15) with y = L as

$$F_R = \frac{GC_p}{U_L} \{1 - \exp(-U_L F'/GC_p)\} \qquad (2.16)$$

The total useful energy gain of the collector can be found from equation (2.16)

$$Q_u = A_P F_R \{S - U_L(T_{f,i} - T_a)\} \qquad (2.17)$$

and instantaneous collector efficiency, η , is defined as:

$$\eta \; = \; \frac{Q_u}{IA_p} \tag{2.18}$$

where I is the total solar radiation on a tilted surface and A_p is the absorber area.

Optical Effects

Basically the same analysis is applicable to the evacuated glass tube solar collectors which has been used for flat plate collectors.

The transmittance for a single glass cover neglecting absorption is

$$\tau_{r,1} \; = \; (1 - \rho)^2 \sum_{n=0}^{\infty} \rho^{2n} \; = \; \frac{(1 - \rho)^2}{1 - \rho^2} = \frac{1 - \rho}{1 + \rho} \tag{2.19}$$

where reflectance

$$\rho(\theta) \; = 1/2 \left[\frac{\sin^2(\theta_2 - \theta_1)}{\sin^2(\theta_2 - \theta_1)} + \frac{\tan^2(\theta_2 - \theta_1)}{\tan^2(\theta_2 + \theta_1)} \right] \tag{2.20}$$

θ_1 and θ_2 in equation (2.20) are the angle of incidence and refraction and by Snell's law

$$\frac{n_1}{n_2} = \frac{\text{Sin } \theta_2}{\text{Sin } \theta_1} \qquad (2.21)$$

n_1 and n_2 in equation (2-21) are refractive indices of the medium.

If the angle of incidence and refractive indices are known, equation (2-20) and (2-21) are sufficient to calculate the reflectance of the single cover, and thus transmittance can be obtained from Equation (2-19).

The absorption of radiation in a partially transparent medium is given by

$$\tau_a = e^{-KL} \qquad (2-22)$$

Where K is the extinction coefficient and is assumed to be a constant in the solar spectrum, L is the actual path of the radiation through the medium.

If the product KL is small, the transmittance allowing for both reflection and absorption is

$$\tau = \tau_{r,1}\, \tau_a \qquad (2-23)$$

$$\tau = e^{-KL}\left(\frac{1 - \rho}{1 + \rho}\right) \qquad (2-24)$$

Using K = 0.2/inch. and L = 0.1 inch. and ρ = 0.0434, corresponding to a refractive index for the glass of 1.526.

τ = 0.899 (normal incidence)

As the glass curves, the angle of incidence increases, which means an increase in both L and ρ. Figure 2-3 shows the change in net transmittance for a plane sheet of glass. Averaging these transmittances over angles to 75 degrees to cover the useful areas of transmission of the glass cylinder[16] gives

$\tau_{avg.}$ = 0.852

If α is the absorptivity of the surface, thermal energy captured by the absorber plate of the collector is

$$S = (\tau\alpha)I \qquad\qquad (2\text{-}25)$$

where I is the total solar radiation on a tilted surface.
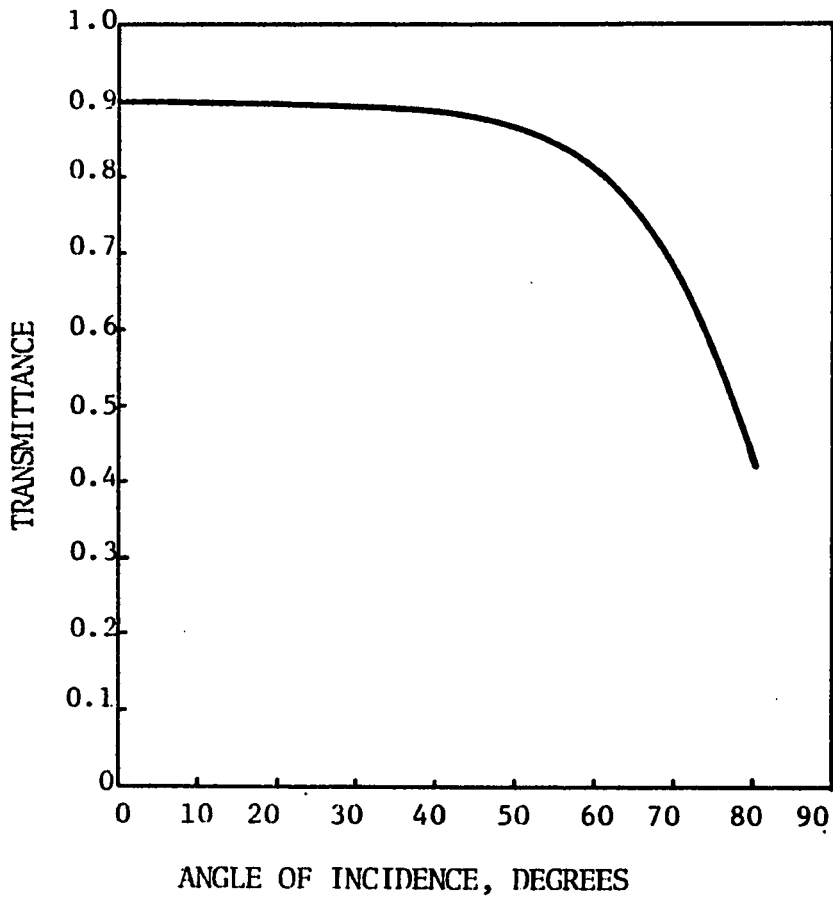
Figure 2.3: Transmittance versus angle of incidence for glass.

The total solar radiation includes the direct
radiation and the diffuse. Using I in equation (2-7)
overstates the received insolation slightly because
the diffuse does not come from the same angle as the
direct. Effect of even lower order that tends to
decrease the incoming radiation is due to shading
by adjacent tubes. However, compensating effects that
serve to increase the received radiation may be due
to internal reflections in the tube, reflections from
adjacent tubes and reflections from the surface behind
the tubes.

CHAPTER III

CALCULATION OF THERMAL LOSSES

Heat is lost from the outside of the glass cylinders by both radiation and convection, but from the absorber to the glass, only radiation transfers the heat, as the heat lost by both convection and conduction are made negligible by evacuation (about 10^{-4} mm Hg). Of course, there is a small amount of conduction from the absorber through the structure that supports it away from the glass walls, but this effect has been neglected. The heat lost by the collector is given by equation (3.1).

$$Q_L = U_L A_p (T_p - T_a) \tag{3.1}$$

The heat transfer coefficient U_L is calculated from the thermal resistance between the collector plate and glass tube and between the glass tube and the exterior as

$$U_L = \{ 1/(h_{g,r} + h_{wp}) + 1/h_{p,r} \}^{-1} \tag{3.2}$$

22

Radiation from the glass cylinder

The radiative loss from the glass tube surface accounts for radiation exchange with the sky at temperature T_s. For simplicity, it is referenced to the ambient air temperature so that the radiation heat transfer coefficient from the cylindrical glass surface can be written as

$$h_{g,r} = \varepsilon_g \sigma \, (T_g^4 - T_s^4)/(T_g - T_a) \qquad (3.3)$$

where ε_g is the emissivity of the glass

σ is the Stefan-Boltzmann Constant 5.6697×10^{-8} W/m² °K⁴

T_g is the temperature of the glass tube, °K

T_a is the ambient air temperature, °K

T_s is the equivalent sky temperature as a function of the ambient air temperature, °K

Swinbank[9] relates sky temperature to the local air temperature in the simple relationship

$$T_{sky} = 0.0552 \, T_{air}^{1.5} \qquad (3.4)$$

The actual radiating surface of each cylinder
is equal to its surface area, but, in effect, much
of the view of each cylinder is the neighbouring
cylinder or the building structure behind the cylinder.
Assuming these surfaces beside and behind the cylinder
to be at the same temperature as the glass, heat is
radiated only to the front. Therefore the area for
radiation of $h_{g,r}$, equation (3.3) is assumed to be
the product of the cylinder diameter and length[16], $D_g L$.
To reference the loss to the absorber equation (3.3) is
multplied by $(D_g L/A_p)$.

Surface Convection

The convection heat transfer coefficient h_{wp} on
the glass tube surface is approximated by heat transfer
coefficient around a cylinder. Expressions for h_w have
been determined from data illustrated by Holman[17, 18]
for single cylinders, namely.

for the case of natural convection and

$$h_w = 1.32 \left(\frac{\Delta T}{D_o}\right)^{0.25}$$

in the case of forced convection for $R_e > 400$

$$h_w = \frac{1}{D_o} (0.0161 \; R_e^{0.492} + 0.007) \qquad (3.5)$$

in SI units, where

$$R_e = 72770 \; D_o W$$

The value of h_w represents the loss per unit area of glass surface. For consistency, all losses are referenced to the net collector area A_p, so h_w is multiplied by (A_g/A_p) before combining with radiation losses below in equation (3-2). Also for a bank of tubes, the loss per tube is less than for a single exposed tube, so 60 percent of the loss rate (h_w) was used as the convection loss rate from the glass surface to air[16]. The adjusted wind loss coefficient is

$$h_{wp} = (A_g/A_p) \; x \; 0.6 \; x \; h_w \qquad (3.6)$$

Radiation From Absorber to Glass

The radiation heat transfer coefficient between the absorber plate and glass tube can be written as

$$h_{p,r} = \epsilon_{pg}\sigma \, (T_p^4 - T_g^4)/(T_p - T_g) \qquad (3.7)$$

where $\qquad \epsilon_{pg}$ the effective emissivity between the absorber plate and the glass is

$$\epsilon_{pg} = (\frac{1}{\epsilon_p} + \frac{A_p}{A_g} (\frac{1}{\epsilon_g} - 1))^{-1} \qquad (3.8)$$

The overall thermal loss coefficient can be obtained by combining equations (3.2), (3.3), (3.6) and (3.7).

The glass temperature T_g is found by noting that the heat loss from the plate to the cover is the same as from the plate to the surroundings. Therefore,

$$T_g = T_p - \frac{U_L(T_p - T_a)}{h_{p,r}} \qquad (3.9)$$

The procedure is to guess a glass temperature from which $h_{g,r}$ and $h_{p,r}$ are calculated. With these heat transfer coefficients and h_{wp}, the overall heat transfer coefficient is calculated from equation (3.2). These results are then used to calculate T_g from equation (3.9). If T_g is close to the initial guess, no further calculations are necessary. Otherwise, the newly calculated T_g is used and the process is repeated.

The values of U_L are shown in Figure 3.1 for
an average absorber emissivity of 0.1. One of the designs
proposed by Corning has an absorber with a front surface
emissivity of about 0.2 and a polished surface on the
back with an emissivity less than 0.05. The average
between the front and back surfaces may be used in
equation (3.8). Several conclusions can be drawn from
the data in Figure 3.1.

1.   Since U_L varies from 1.1 to 2.0 W/m²°C in
        the potential operating temperature range of
        the collector, the collector can be described
        as having a very low loss coefficient.

2.   The U_L value increases gradually with
        increasing operating temperatures. It is
        undesirable to operate the collector at a
        large temperature gain in one pass because of
        the decrease in performance as can be seen
        later. If the collector is operated at a modest
        temperature gain, U_L can be treated as a constant
        over this temperature range. Thus, linear theory
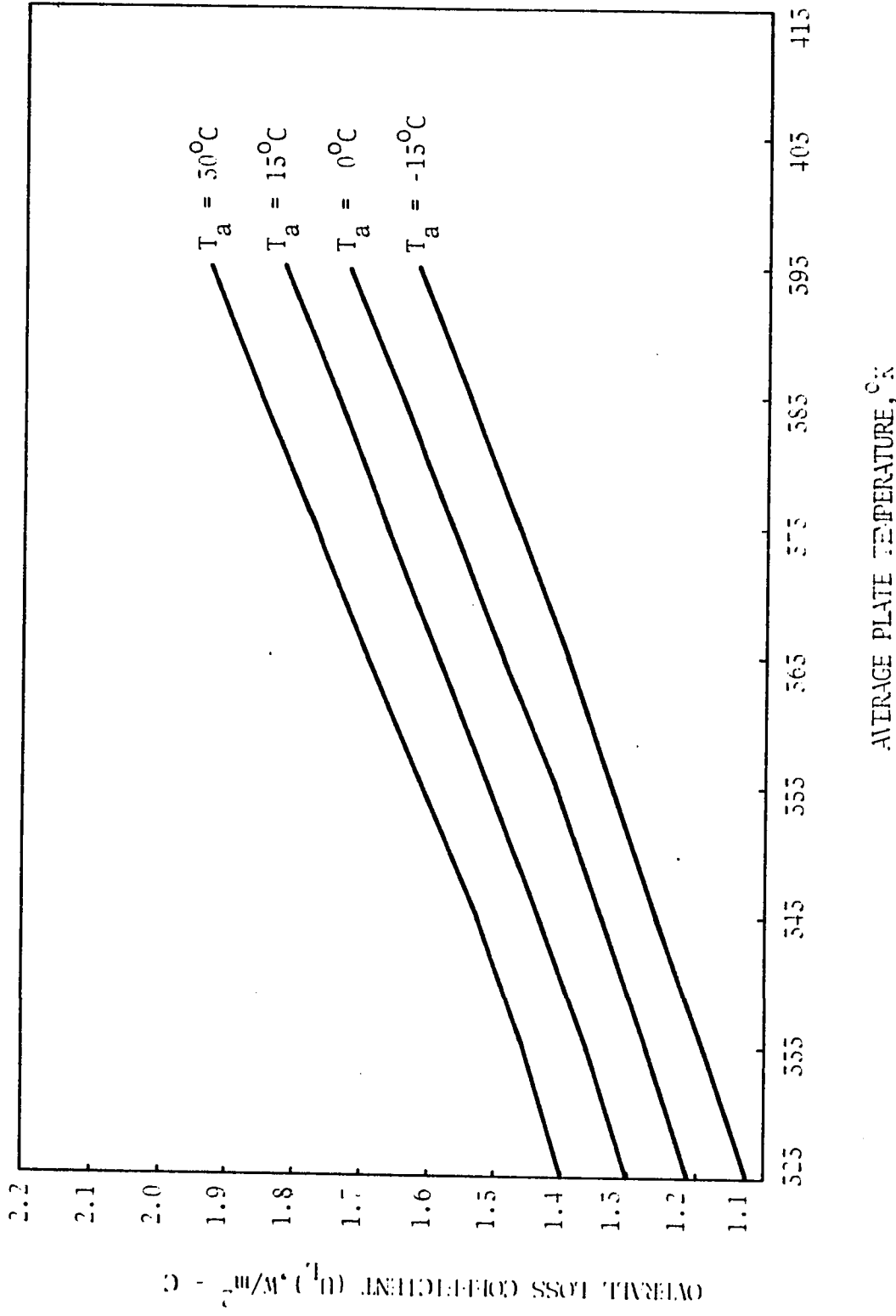   in heat balance calculations can be used.

Figure 5.1: Overall loss coefficient for evacuated tubular collector, for emissivity 0.1 and V = 5m s.

3.   The overall loss coefficient decreases somewhat
with decreasing ambient temperature because
the value of U_L is controlled by radiation
loss from the collector. This is important
in heating season applications where the
ambient temperature is low.

4.   Because of the low loss coefficient, liquids
as well as gases can be used as the working
fluid. Even though the heat transfer from the
absorber tube to the working fluid is much
poorer with gases than with liquids, the
consequent rise in absorber surface temperature
does not increase the heat loss appreciably.

Loss rates, U_L, were also computed for average
absorber emissivities of 0.3, 0.5, 0.7 and 0.9, and these
values are shown in Figure 3.2 in relation to loss rates
for emissivity of 0.1. It is apparent from these results
that, to very good approximation U_L is proportional to
emissivity for these evacuated collectors. Therefore for
emissivities other than 0.1, the value of U_L from Figure 3.1
may be adjusted by the ratio of the average emissivity
to 0.1.
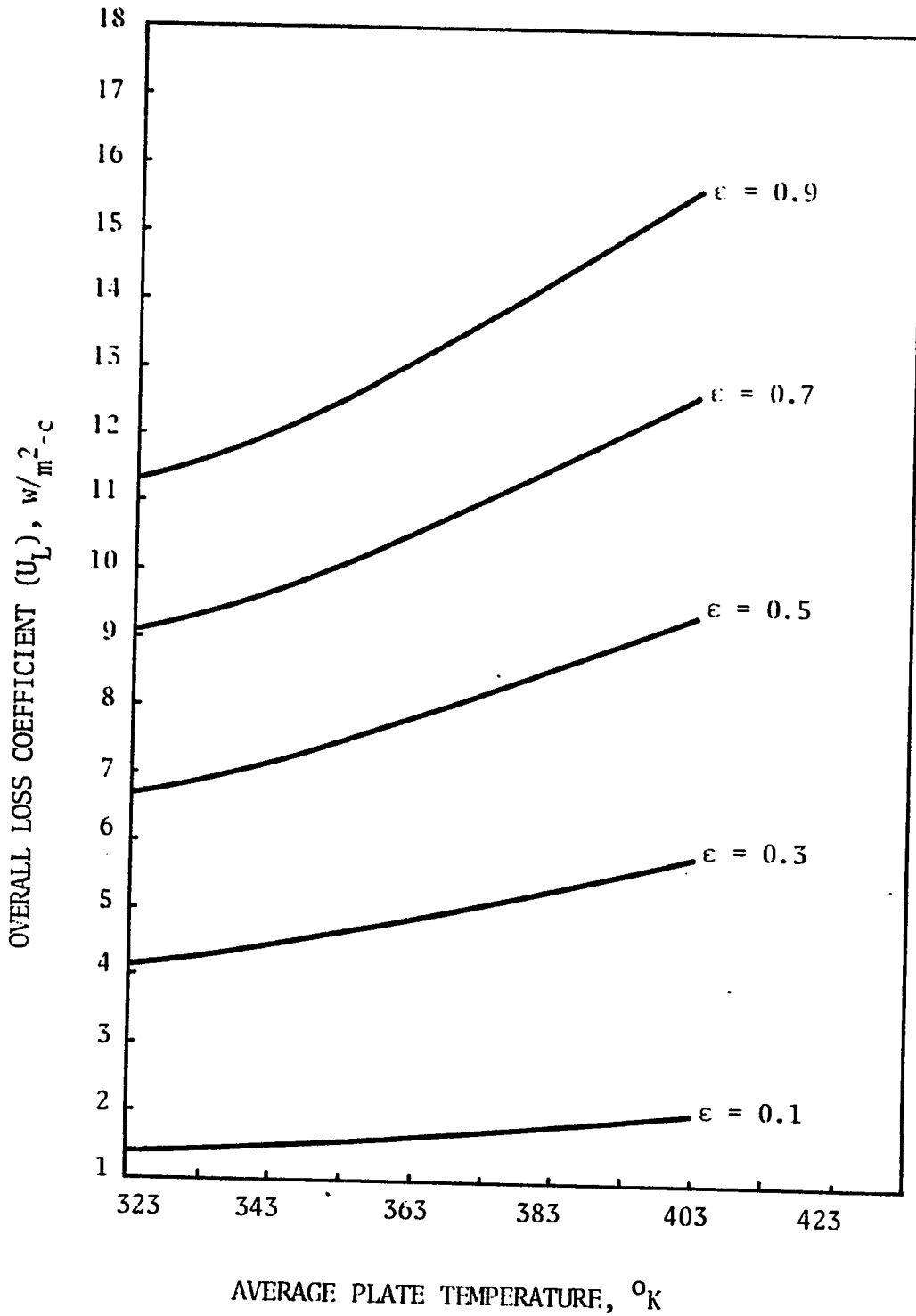
Figure 3.2: Overall loss coefficient versus average
plate temperature and emissivity for
$T_a = 30^\circ C$ and $V = 5$ m/s.

Figure 3.3 shows the computed glass temperature for several values of plate emissivity. For an emissivity of 0.1 the heat loss through the collector is so small that the glass tube temperature is within a few degrees of ambient temperature even at high absorber temperatures. As emissivity increases the glass temperature increases. This means that U_L is most strongly dependent on the radiation loss coefficient $h_{p,r}$.

Figure 3.3: Glass temperature versus absorber temperature and emissivity for v = 5m/s and T_a = 30°C.

CHAPTER IV

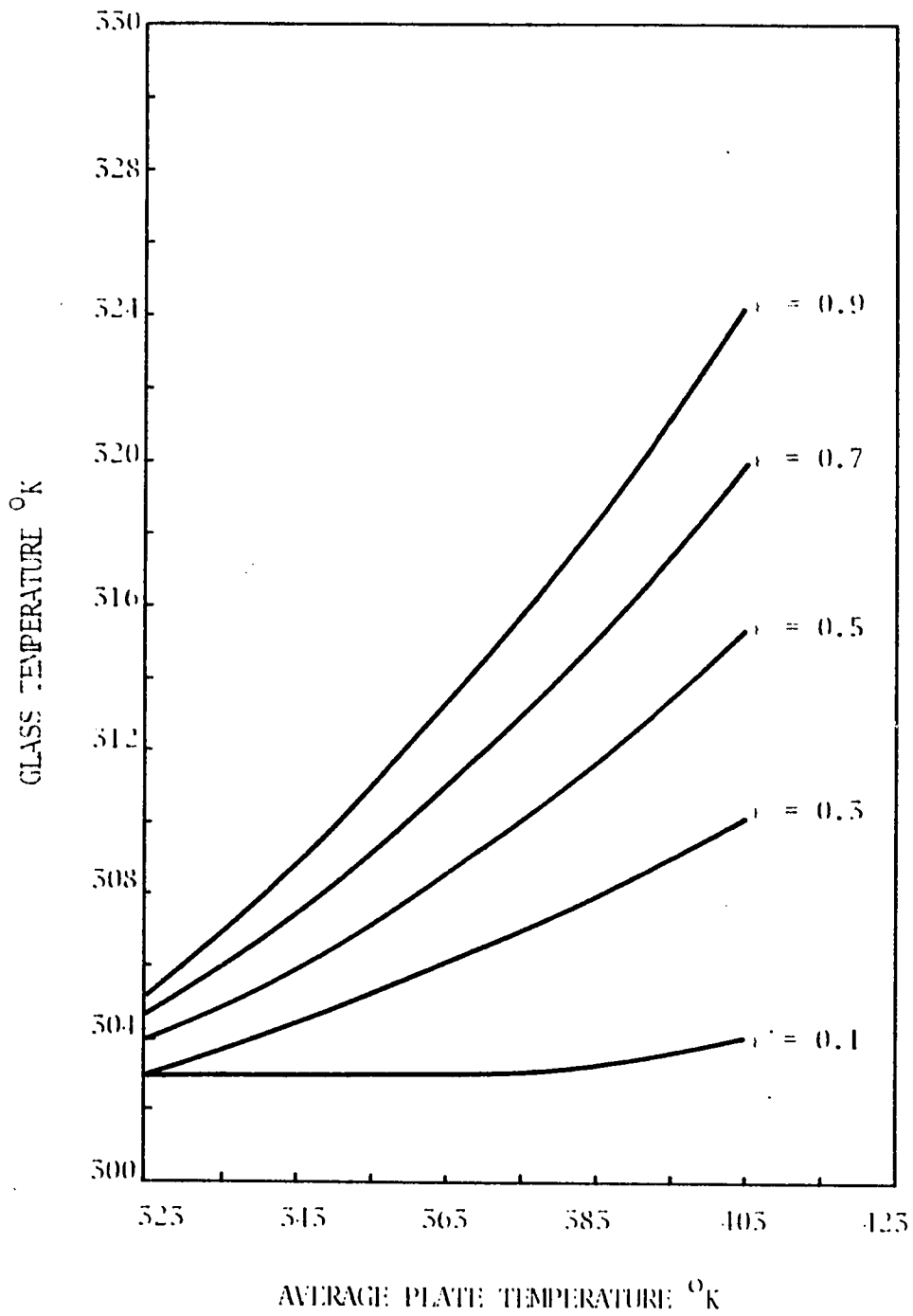## TWO DIMENSIONAL PROBLEM FORMULATION
AND SOLUTION

Governing Equations

A steady state analysis is made on a portion of
a collector consisting of a single tube with a fin attached
to it as shown in Figure 4.1. All the assumptions used
in the one-dimensional collector model of chapter
II are retained in the present analysis except assumption
10, i.e., the assumption that axial conduction in the
absorber plate does not effect the plate conductance
for transverse heat flow. Here it is assumed that the
temperature distribution in the plate is two-dimensional
and temperature gradient along the tube thickness is
negligible. For the fluid inside the tube, radial
variation of temperature is neglected. Although it is
known that the overall heat loss coefficient from the
plate to the surroundings is a function of the local
plate temperature, an average value of this coefficient
valid for the whole plate is used. This average value is
estimated iteratively using expression developed[9] for
thermal losses in chapter III and the expression for the
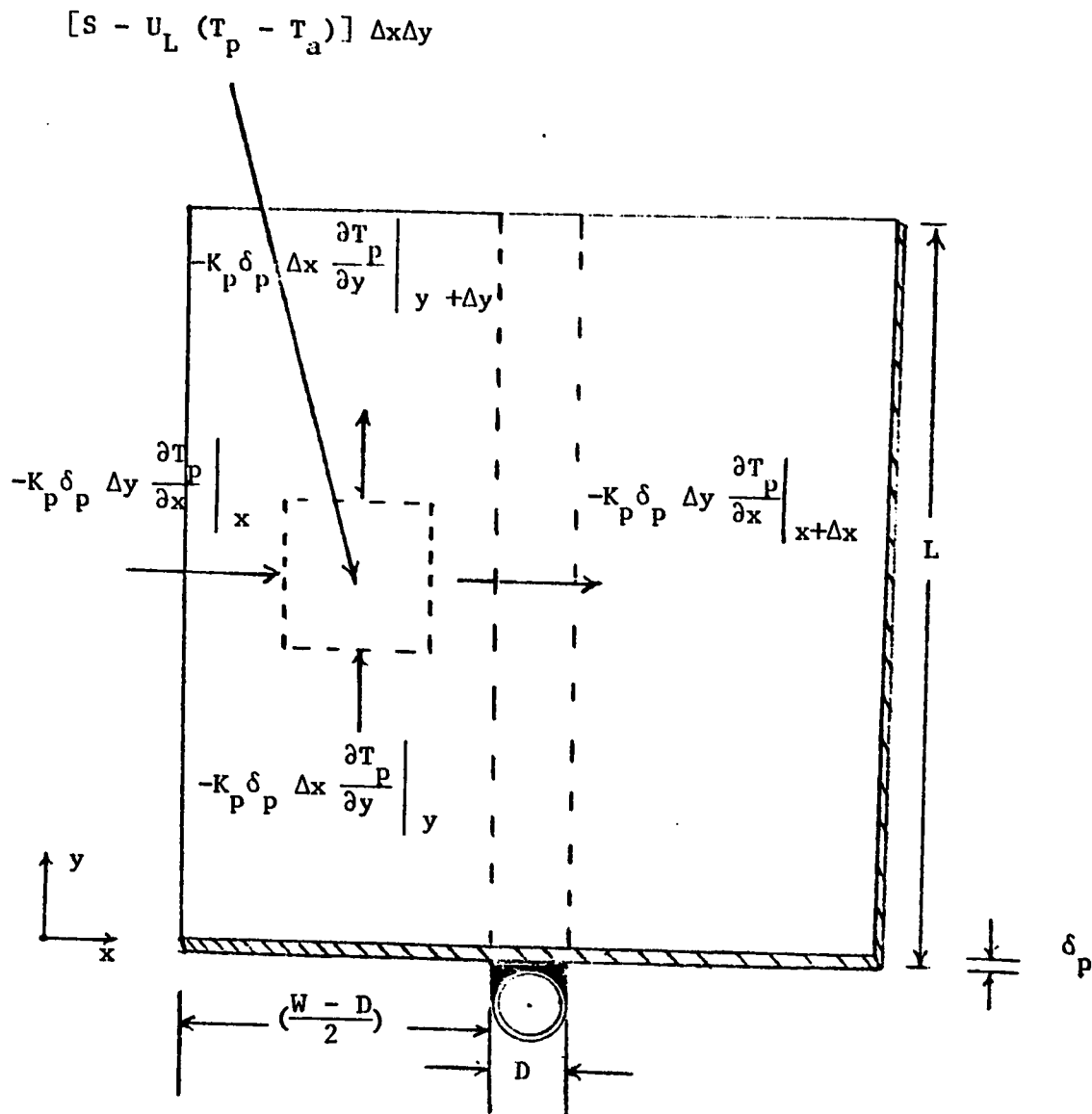
Figure 4.1: Absorber plate section.

average plate temperature. Energy balances are made
on absorber plate and tube each considered as a separate
unit and two differential equations are obtained in the
following manner.

Absorber Plate

A two-dimensional control-volume on the absorber
plate, valid for $0 \leqslant x \leqslant (W-D)/2$ and $0 \leqslant Y \leqslant L$ is
shown in Figure 4.1. An energy balance on the control
volume yields the following governing equation.

$$K_p \delta_p \frac{\partial^2 T_p}{\partial x^2} + K_p \delta_p \frac{\partial^2 T_p}{\partial Y^2} + S - U_L(T_p - T_a) = 0 \qquad (4.1)$$

where $T_p = T_p(x, y)$

Introducing dimensionless variables

$$x^* = x/(\frac{W - D}{2})$$

$$y^* = Y/L$$

$$T_p^*(x^*, y^*) = \frac{\theta_p}{\theta_{f,i}}$$

Where

$$\theta_p(x,y) = \{T_p(x,y) - T_a - S/U_L\}$$

and $\quad \theta_{f,i} = \{T_{f,i} - T_a - S/U_L\}$

Equation (4.1) now becomes

$$\frac{\partial^2 T^*_p}{\partial x^{*2}} + P^2 \frac{\partial^2 T^*_p}{\partial Y^{*2}} - Q^2 T^*_p = 0 \qquad (4.2)$$

where $\quad P = (\frac{W - D}{2}) \cdot \frac{1}{L}$

$$Q^2 = \frac{U_L (\frac{W - D}{2})^2}{k_p \delta_p}$$

Equation (4.2) is the governing differential equation for the absorber plate.

Fluid Inside the Tube

An energy balance on the fluid element Δy shown in Figure 2.2 yields

$$\dot{m} c_p \frac{dT_f}{dy} = q_u(y) \qquad (4.3)$$

or $\qquad \dot{m}C_p \dfrac{dT_f}{dy} = [T_p(\dfrac{W - D}{2}, y) - T_f] /R$ $\qquad\qquad$ (4.4)

where $\quad T_f = T_f(y)$

Introducing dimensionless variables

$\qquad T_f^* = \dfrac{\theta_f}{\theta_{f,i}}$ $\quad$ where $\theta_f(y) = \{T_f(y) - T_a - S/U_L\}$

Equation (4.4) becomes

$\qquad \dfrac{\dot{m}C_p}{L} \dfrac{dT_f^*}{dy^*} = [T_p^* (1, y^*) - T_f^* (y^*)] /R$ $\qquad$ (4.5)

Rearranging

$\qquad \dfrac{dT_f^*}{dy^*} + fT_f^* - f \; T_p^* (1, y^*) = 0$ $\qquad\qquad$ (4.6)

where $\quad f = L/R \; \dot{m}C_p$

This is the governing differential equation for the fluid.

Boundary Conditions

For the absorber plate region, there are three
homogeneous and one non-homogeneous boundary conditions.
In an evacuated tubular collector, we can assume that
the heat loss at the boundaries $y = 0$ and $y = L$ and at
the sides of the plate is negligibly small. Also the
boundary $x = 0$ is the midpoint of plate between two
adjacent tubes, symmetry requires that the slope of
the temperature be zero at this boundary. The non-homogeneous
boundary condition at $x = (W-D)/2$ is given by an
energy balance on the tube base region. These boundary
conditions can now be expressed as:

1.   At $y = 0$ $\dfrac{\partial T_p}{\partial y} = 0$ (4.7)

2.   At $y = L$ $\dfrac{\partial T_p}{\partial y} = 0$ (4.8)

3.   At $x = 0$ $\dfrac{\partial T_p}{\partial x} = 0$ (4.9)

4.   At $x = \dfrac{W - D}{2}$

$$- 2K_p \delta_p \left. \frac{\partial T_p}{\partial x} \right|_{x = (W - D)/2} + D \{S - U_L (T_p (\tfrac{W-D}{2}, y) - T_a)\}$$

$$= [T_p (\tfrac{W - D}{2}, y) - T_f]/R \qquad (4.10)$$

The fluid boundary condition is given by specifying the inlet fluid temperature, i.e.,

5. At $y = 0$ $T_f = T_{f,i}$ $\qquad\qquad$ (4.11)

Non-dimensionalizing the variables, the boundary condition can be rewritten in the following way:

1. At $y^* = 0$ $\dfrac{\partial T_p^*}{\partial y^*} = 0$ $\qquad\qquad$ (4.12)

2. At $y^* = 1$ $\dfrac{\partial T_p^*}{\partial y^*} = 0$ $\qquad\qquad$ (4.13)

3. At $x^* = 0$ $\dfrac{\partial T_p^*}{\partial x^*} = 0$ $\qquad\qquad$ (4.14)

4. At $x^* = 1$

$$\frac{\partial T_p^*}{\partial x^*} + (g + h) T_p^* = g T_f^* \qquad (4.15)$$

where $g = (W - D)/w \, K_p \, \delta_p R$

$h = DU_L (W - D)/4K_p \delta_p$

And for the fluid

5.   At $y^* = 0$ $T_f^* = 1$ (4.16)

Temperature Distribution of the Absorber Plate

The dimensionless, linear and homogeneous differential equation obtained in equation (3.2) is:

$$\frac{\partial^2 T_p^*}{\partial x^{*2}} + P^2 \frac{\partial^2 T_p^*}{\partial y^{*2}} - Q^2 \, T_p^* = 0 \qquad (4.2)$$

We now seek a solution by the method of separation of variables.

Assume a product solution of the form

$$T_p^* (x^*, y^*) = X(x^*) \; Y \; (y^*) \qquad (4.17)$$

and substituting into equation (4.2)

$$\frac{X''}{X} + P^2 \frac{Y''}{Y} - Q^2 = 0 \qquad (4.18)$$

or $\qquad \frac{X''}{X} - Q^2 = - P \frac{Y''}{Y} = \pm \lambda^2 \qquad (4.19)$

where $\pm \lambda^2$ is an arbitrary constant. Here the sign of λ^2 must be chosen such that the homogeneous $y*$-direction results in a characteristics-value problem[19], hence $+\lambda^2$ is suitable to this problem.

Finally, we have the problem separately expressed in the $x*$ and $y*$-directions as follows:

$$\frac{X''}{X} - Q^2 = \lambda^2 \qquad (4.20)$$

$$-P^2 \frac{Y''}{Y} = \lambda^2 \qquad (4.21)$$

Rearranging

$$Y'' + \lambda*^2 Y = 0 \qquad (4.22)$$

$$X'' - \gamma^2 X = 0 \qquad (4.23)$$

where $\lambda^* = \lambda/P$

$$\gamma^2 = \lambda^2 + Q^2$$

The general solutions to these two ordinary differential equations are

$$Y(y^*) = A \, Cos(\lambda^* y^*) + B \, Sin(\lambda^* y^*) \qquad (4.24)$$

$$X(y^*) = C \, Sinh(\gamma x^*) + D \, Cosh(\gamma x^*) \qquad (4.25)$$

The form of solution assumed in equation (4.17) will now become

$$T_P^*(x^*, y^*) = (A \, Cos(\lambda^* y^*) + B \, Sin \, (\lambda^* y^*))(C \, Sinh \, (\gamma x^*)$$
$$+ D \, Cosh(\gamma \, x^*)) \qquad (4.26)$$

Application of the homogeneous boundary conditions (1) and (2)

$$\left. \frac{dY}{dy^*} \right|_{y^* = 0} = 0 \qquad \text{and} \quad \left. \frac{dY}{dy^*} \right|_{y^* = 1} = 0$$

Equation (4.24) yields a family of solutions, i.e.,

$$Y_n(y^*) = A_n \cos \lambda_n^* y^* \quad n = 0, 1, 2, \ldots \quad (4.27)$$

where $\lambda_n^* = \lambda_n/P = n\pi$ and A_n is an arbitrary constant.

Applying boundary condition (3).

$$\left. \frac{dx}{dx^*} \right|_{x^* = 0} = 0$$

to equation (4.25) yields

$$X_n(x^*) = E_n \cosh (\gamma_n x^*) \quad (4.28)$$

where $\gamma_n = \lambda_n^2 + Q^2$

Equation (4.26) can now be written as

$$T_p^* (x^*, y^*) = \sum_{n=0}^{\infty} A_n E_n \cosh \gamma_n x^* \cos \lambda_n^* y^*$$

or

$$T_p^* (x^*, y^*) = \sum_{n=0}^{\infty} C_n \cosh \gamma_n x^* \cos \lambda_n^* y^* \quad (4.29)$$

Where C_n represents the product $A_n E_n$. C_n's are still unknown and have to be determined using the fourth non-homogeneous boundary condition. Equation (4.29) gives the plate temperature distribution.

From equation 4.15 the fourth boundary condition is

$$\left. \frac{\partial T_p^*}{\partial x^*} \right|_{x^*=1} + (g + h)T_p^* \, (1, \, y^*) = g \, T_f^*(y^*) \qquad (4.15)$$

From equation (4.29)

$$\left. \frac{\partial T_p^*}{\partial x^*} \right|_{x^*=1} = \sum_{n=0}^{\infty} C_n \, \gamma_n \, \text{Sinh} \, \gamma_n \, \text{Cos} \, \lambda_n^* y^* \qquad (4.30)$$

Substituting equation(4.30)in quation(4.15)gives

$$\sum_{n=0}^{\infty} C_n \{\gamma_n \, \text{Sinh} \, \gamma_n + (g + h)\text{Cosh} \, \gamma_n\} \, \text{Cos} \, \lambda_n^* \, y^*$$

$$= gT_f^* \, (y^*) \qquad (4.31)$$

An expression for T_f^*, which is the temperature distribution of the fluid has to be substituted before $C_n's$ can be evaluated.

Temperature Distribution of the fluid

The dimensionless differential equation of the fluid obtained in equation (4.6) is:

$$\frac{dT_f^*}{dy^*} + f \ T_f^* - f \ T_p^*(1, \ y^*) = 0 \qquad (4.6)$$

Using equation (4.29), quation (4.6) can be written as

$$\frac{dT_f^*}{dy^*} + f \ T_f^* = f \sum_{n=0}^{\infty} C_n \ \text{Cosh} \ \gamma_n \ \text{Cos} \lambda_n^* y^* \qquad (4.32)$$

The solution to this differential equation using the method of integrating factors is:

$$T_f^*(y^*) = e^{-fy^*} [f \sum_{n=0}^{\infty} C_n \text{Cosh} \ \gamma_n \{ \frac{e^{fy^*}}{(f^2 + \lambda_n^{*2})}$$

$$(f \cos \lambda_n^* y^* + \lambda_n^* \ \text{Sin} \ \lambda_n^* y^*) \} + F \ ] \qquad (4.33)$$

Applying the boundary condition

At $y^* = 0$ $\qquad T_f^* = 1$

We obtain

$$F = 1 - \sum_{n=0}^{\infty} C_n \ \text{Cosh} \ \gamma_n/(1 + \xi_n^2) \qquad (4.34)$$

where $\xi_n = \lambda_n^*/f$

Substituting the value of F in equation(4.33)gives fluid temperature distribution as

$$T_f^*(y^*) = e^{-fy^*} + \sum_{n=0}^{\infty} \frac{C_n \ \mathrm{Cosh} \ \gamma_n}{(1 + \xi_n^2)} \{ \ \mathrm{Cos} \ \lambda_n^* y^* + \xi_n \mathrm{Sin} \ \lambda_n^* y^*$$
$$- e^{-fy^*} \} \qquad (4.35)$$

The coefficients $C_n's$ can now be evaluated substituting equation (4.35) in equation(4.31)

$$\sum_{n=0}^{\infty} C_n \{ \ \gamma_n \mathrm{Sinh} \ \gamma_n + (g + h) \ \mathrm{Cosh} \gamma_n \ \} \mathrm{Cos} \ \lambda_n^* y^* =$$

$$g \ [e^{-fy^*} + \sum_{n=0}^{\infty} \frac{C_n \mathrm{Cosh} \gamma_n}{(1 + \xi_n^2)} \{ \mathrm{Cos} \ \lambda_n^* y^* + \xi_n \mathrm{Sin} \lambda_n^* y^*$$
$$- e^{-fy^*} \}] \qquad (4.36)$$

Rearranging

$$\sum_{n=0}^{\infty} C_n \ [V_n \mathrm{Cos} \lambda_n^* y^* - U_n \{ \ \mathrm{Cos} \lambda_n^* y^* + \xi_n \mathrm{Sin} \lambda_n^* y^* - e^{-fy^*} \}]$$
$$= g e^{-fy^*} \qquad (4.37)$$

or $\qquad \sum_{n=0}^{\infty} C_n \phi_n(y^*) = g\ e^{-fy^*}$ $\qquad\qquad$ (4.38)

where $\quad V_n = \gamma_n Sinh\gamma_n + (g + h)\ Cosh\gamma_n$

$$U_n = g\ \frac{Cosh\gamma_n}{1 + \xi_n^2}$$

and $\quad \phi_n(y^*) = V_n\ Cos\lambda_n^* y^* - U_n\{\ Cos\lambda_n^* y^* + \xi_n Sin\lambda_n^* y^* - e^{-fy^*}\}$

The problem is to choose C_n's so that equation(4.38) is satisfied identically. Because the functions $\phi_n(y^*)$ are not orthognal, the C_n's cannot be obtained by a Fourier series analysis.

In the computations an approximation is made by means of collocation scheme[20] to obtain these constants. The scheme is discussed in Appendix A.

The plate temperature distribution is now given by:

$$T_p(x^*,y^*) = T_p^*(x^*,y^*)\cdot e_{f,i} + T_a + S/U_L \qquad (4.39)$$

and the fluid temperature distribution is given by:

$$T_f(y^*) = T_f^*(y^*) \; \theta_{f,i} + T_a + S/U_L \qquad (4.40)$$

Average Absorber Plate Temperature

An expression for the average plate temperature can be obtained by integrating the plate temperature distribution over the whole area of the plate.

The temperature distribution of the absorber plate as given by equation (4.29) is:

$$T_p^* = C_0 \; CoshQx^* + \sum_{n=1}^{\infty} C_n Cosh\gamma_n x^* Cos\lambda_n^* \; y^* \qquad (4.29)$$

Integrating this expression over the whole area of the plate

$$T_{pm}^* = \int_0^1 \int_0^1 T_p^* \; (x^*, y^*) \; dx^* \; dy^* \qquad (4.41)$$

or

$$T_{pm}^* = \int_0^1 \int_0^1 [C_0 \; CoshQx^* + \sum_{n=1}^{\infty} C_n \; Cosh\gamma_n x^* Cos\lambda_n^* y^*] \; dx^* dy^*$$

$$T_{pm}^* = \frac{C_0 SinhQ}{Q} \qquad (4.42)$$

The average plate temperature is given by:

$$T_{pm} = T^*_{pm} \quad \theta_{f,i} + T_A + S/U_L \qquad\qquad (4.43)$$

Average Fluid Temperature

An expression for average fluid temperature can be obtained using equation (4.35) as:

$$T^*_{fm} = \int_0^1 T^*_f(y^*) \, dy^* \qquad\qquad (3.44)$$

or

$$T^*_{fm} = \int_0^1 [e^{-fy^*} + (1 - e^{-fy^*})C_0 \, CoshQ + \sum_{n=1}^{\infty} \frac{C_n Cosh\gamma_n}{(1 + \xi_n^2)}$$

$$\{Cos\lambda^*_n y^* + \xi_n Sin\lambda^*_n y^* - e^{-fy^*}\}]dy^*$$

or

$$T^*_{fm} = \frac{1}{f} [(1 - e^{-f}) + \{f - (1 - e^{-f})\} \, C_0 \, CoshQ -$$

$$\sum_{n=1}^{\infty} \frac{C_n Cosh\gamma_n}{(1 + \xi_n^2)} \{(-1)^n - e^{-f}\}] \qquad\qquad (4.45)$$

The average fluid temperature is now given by

$$T_{fm} = T^*_{fm} \, \theta_{f,i} + T_a + S/U_L \qquad\qquad (4.46)$$

CHAPTER V

DISCUSSION OF RESULTS, CONCLUSIONS AND RECOMMENDATIONS

In this chapter, the effects of various parameters on the temperature distributions and instantaneous collector efficiencies are discussed considering a single cylinder. All the simulations were carried out using typical baseline conditions given in Table 5.1 and taking water as a circulating fluid. The results presented will include a comparison to the HWB (Hottel-Whillier-Bliss) model.

Plate Temperature Distribution Parallel to the Tube

The energy transferred to the fluid will gradually heat up the fluid causing a temperature gradient to exist in the direction of flow. Since in any region of the plate, the temperature distribution is governed by the local temperature level of the fluid, a situation as shown in Figure 5.1 exists. Observe that the temperature of the plate midway between the tubes (i.e. @ $x^* = 0$) is higher than at the root (i.e. @ $x^* = 1$) of the plate. The temperature profiles are almost linear.

Plate Temperature Distribution Normal to the Tube

The temperature distribution of one-half the plate between two tubes is shown in Figure 5.2. Some of the solar

Table 5.1

Base-Line Conditions

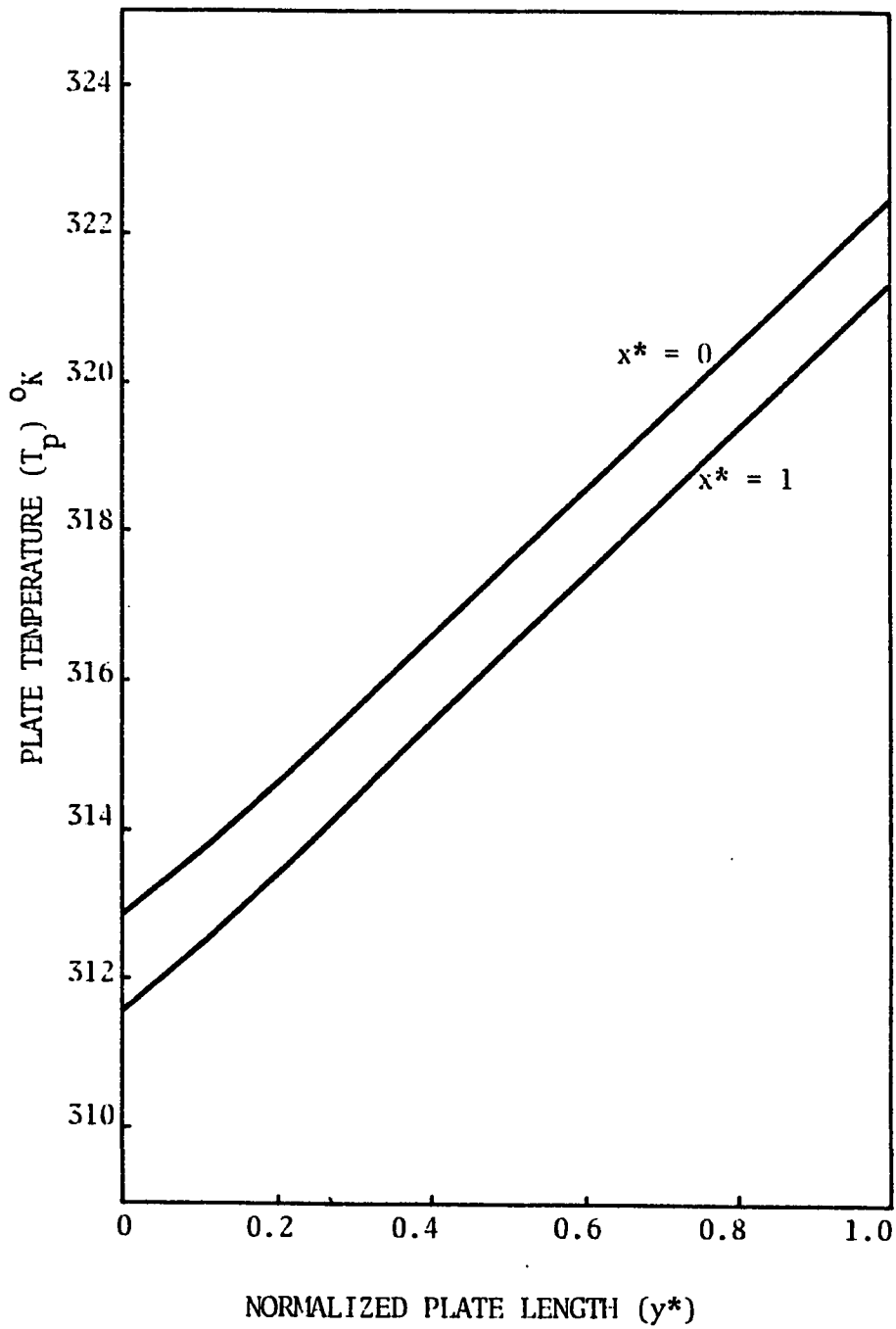|		
Solar Radiation on a Tilted Surface	I =	1100 W/m^2
Ambient Temperature	T_a =	$20^{\circ}C$
Wind Speed	V =	5 m/s
Fluid Inlet Temperature	$T_{f,i}$ =	$35^{\circ}C$
Mass Flow Rate	m =	0.02 kg/s
Absorber Length	L =	2.0 m
Center-to-Center Tube Spacing	W =	0.05 m
Plate Thickness	δ_p =	0.0008 m
Outside Diameter of Flow Channel	D =	0.007 m
Thermal Conductivity	K_p =	$210 W/m^{\circ}K$

Figure 5.1: Plate temperature distribution
parallel to the tube versus
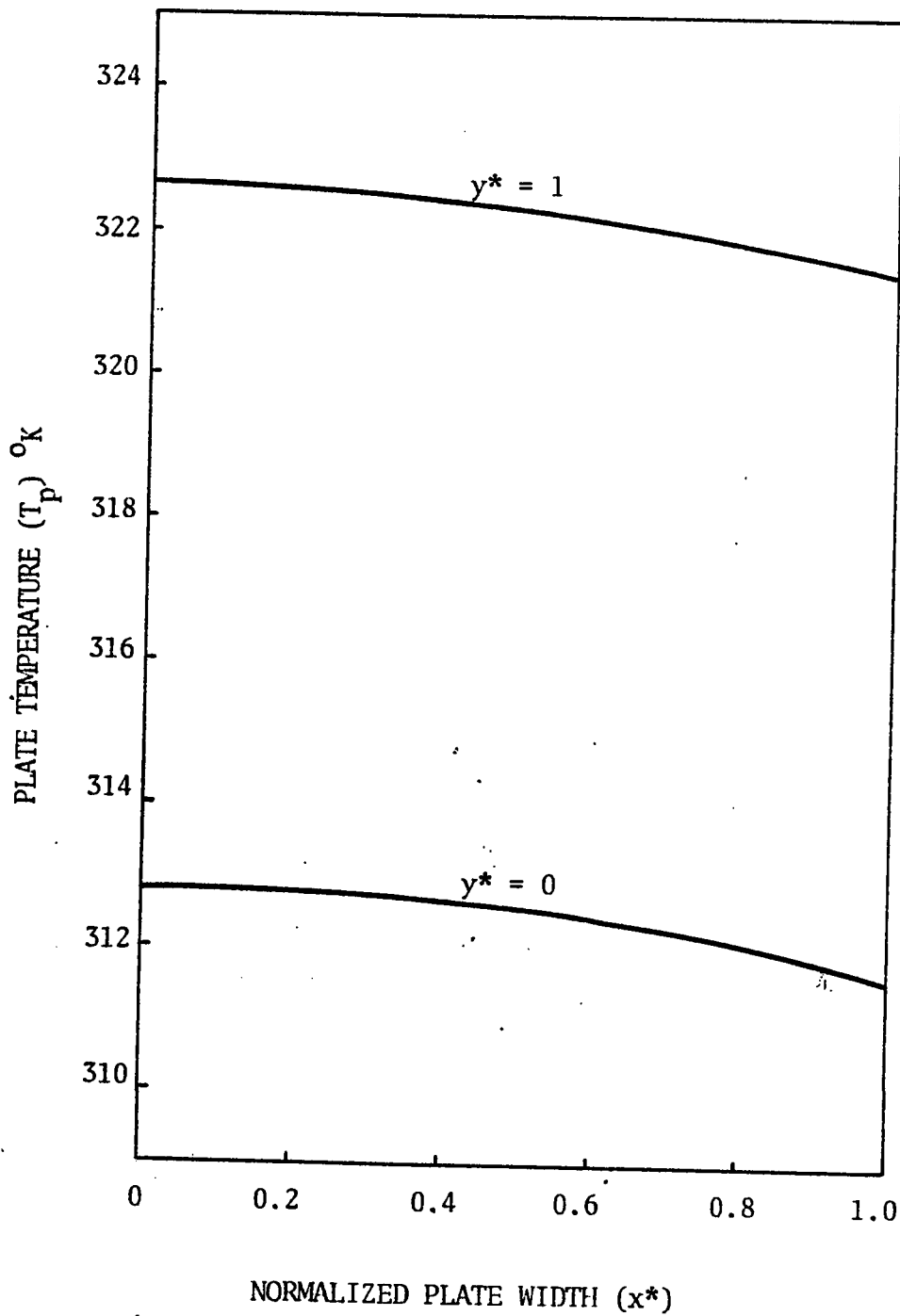normalized plate length for
base-line conditions.

Figure 5.2: Plate temperature distribution
normal to the tube versus normalized
plate width for base-line conditions.

energy absorbed by the plate must be conducted across
the plate to the region of the tubes. Thus the temperature
midway between the tubes will be higher than the
temperature near the tube base region. Observe that the
difference between the center line temperature and
temperature at the tube base region is greater at the
inlet end (i.e. @ $y^* = 0$) than at outlet end (i.e. @ $y^* = 1$).

Isotherms of the Collector Plate

Since the temperature distribution of the absorber
plate obtained in this analysis is two-dimensional, it
can be best illustrated by drawing the isotherms. Figures
5.3 and 5.4 shows the isotherms of an absorber plate
for two different values of mass flow rate. The isotherms
are highly dependent on the mass flow rate. It is interesting
to note that at high flow rate the isotherms are becoming
nearly parallel to the water tube and gradually becomes
normal to the tube for very low flow rate. This means that
at lower flow rates the isotherms show a substantial
component of heat flux parallel to the water tube which
is not accounted for in the HWB model.

Effect of Tube Spacing on Plate Temperature Distribution

Figure 5.5 illustrate the effect of tube spacing
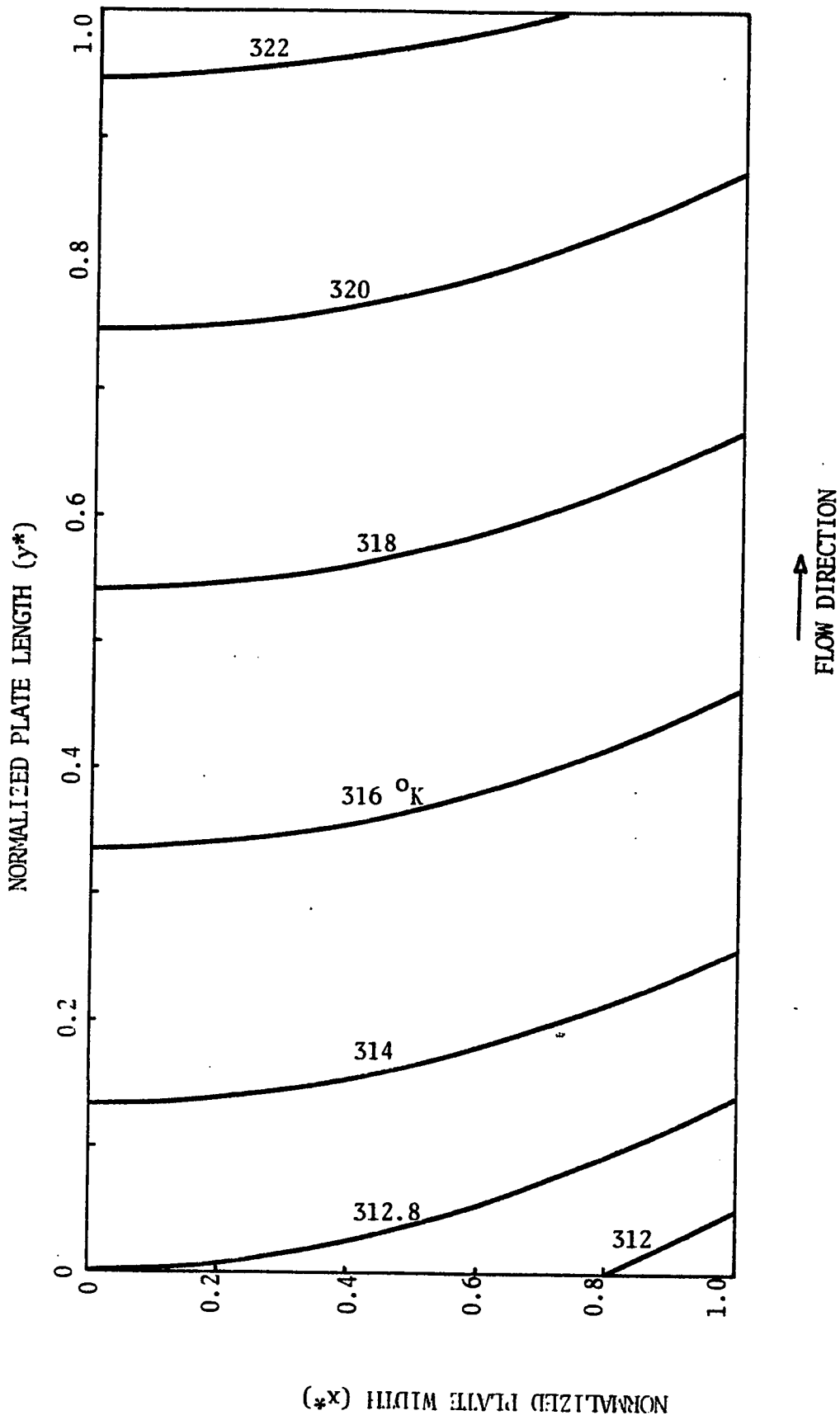on the plate temperature distribution parallel to the

Figure 5.3: Isotherms of the absorber plate for a flow rate of 0.02 kg/$_{s-m}$2 and base-line conditions.
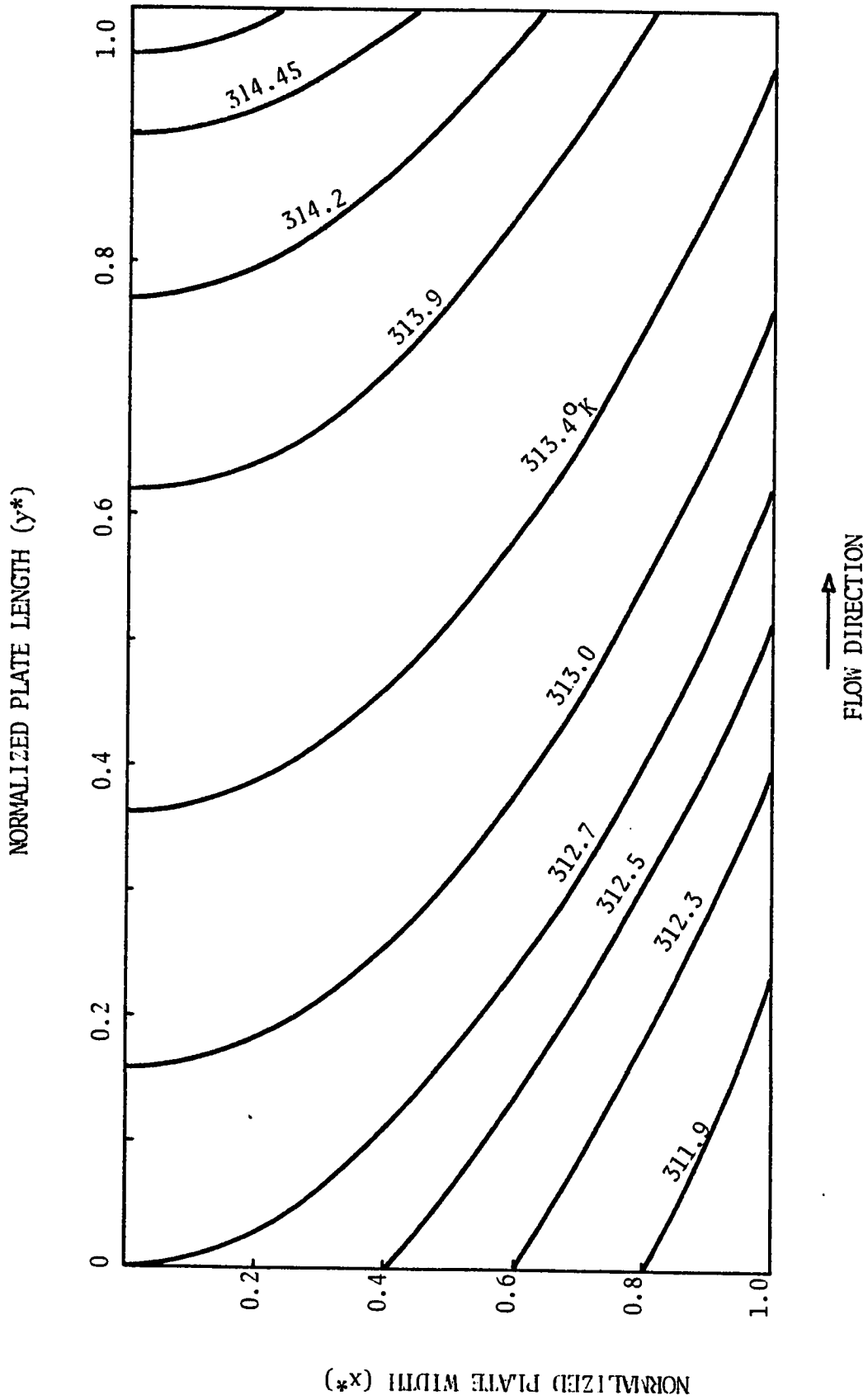
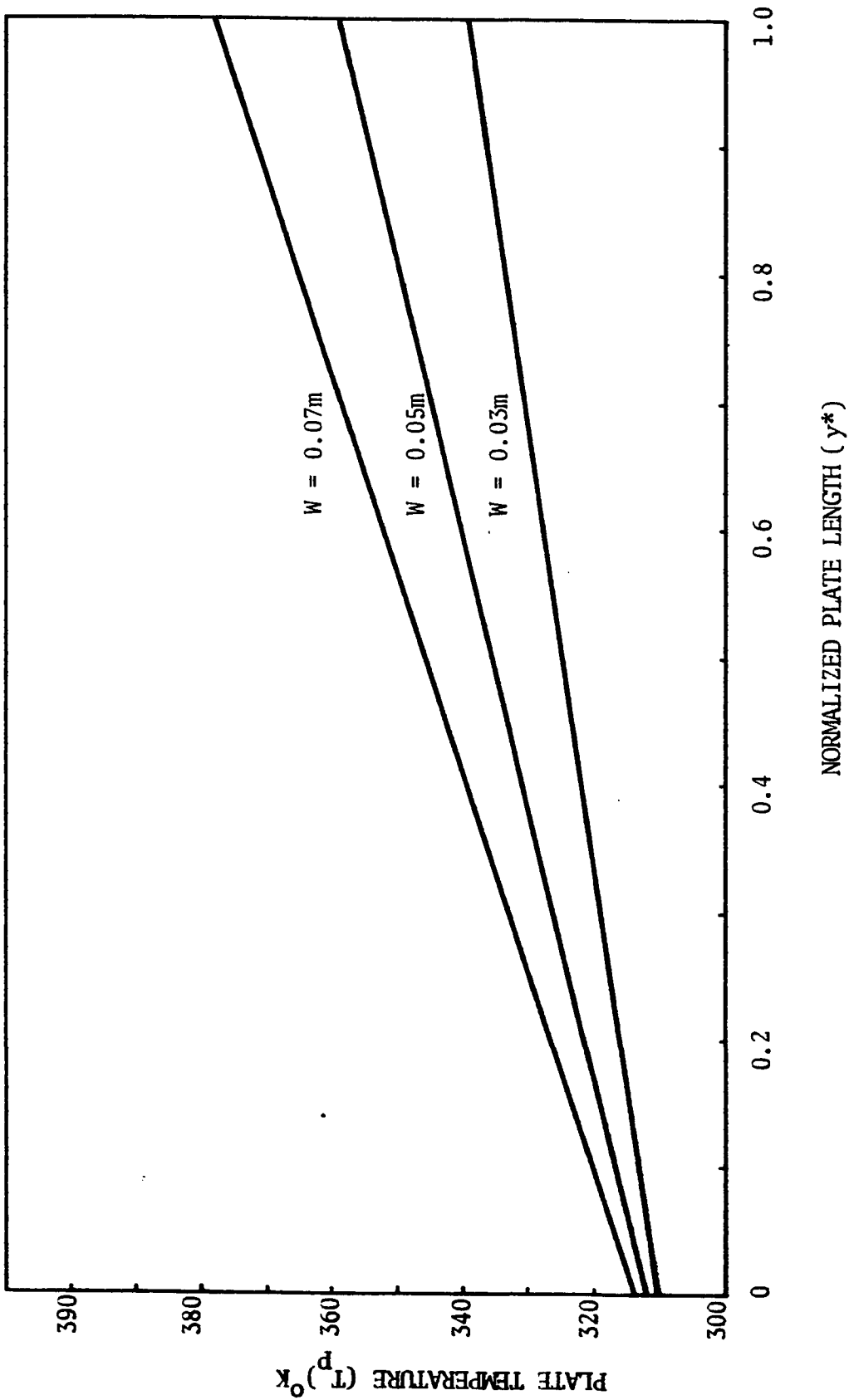Figure 5.4: Isotherms of the absorber plate for a flow rate of 0.1 kg/$_{s-m}$2 and base-line conditions

Figure 5.5: Effect of tube spacing on plate temperature profile parallel to the tube for base-line conditions and x* = 1.

tube. Observe that wider tube spacing results in higher plate temperatures due to an increase in the total amount of energy absorbed by the plate. Figure 5.6 show the effect of tube spacing on the plate temperature distribution normal to the tube. Observe that wider tube spacing results in higher temperature gradients which is due to an increase in the thermal resistance of the plate.

Effect of Tube Spacing on Outlet Fluid Temperature

Figure 5.7 illustrate the effect of tube spacing on outlet fluid temperature. Observe that an increase in tube spacing results in an increase in the fluid outlet temperature.

Effect of Flow Rate on Fluid Temperature Distribution

The temperature distributions of the fluid inside the tube are shown in Figure 5.8 for various mass flow rates. Observe that the temperature profiles are linear for all the three flow rates. Note that for a given length of tube an increase in mass flow rate results in a decrease in fluid temperatures.

Effect of Flow Rate on Fluid Outlet Temperature

Figure 5.9 illustrate effect of mass flow rate on outlet fluid temperature. Broken line shows the outlet
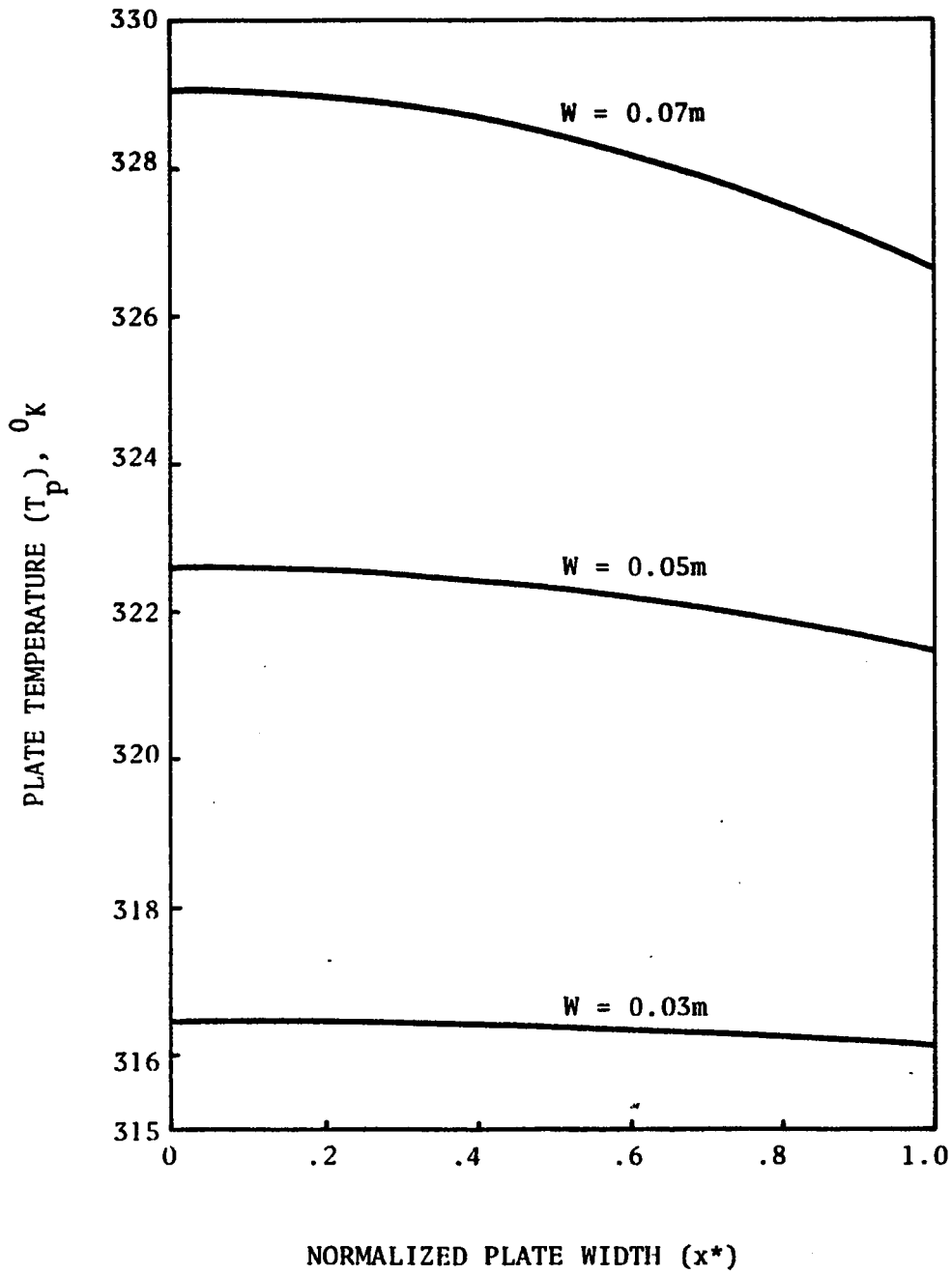
NORMALIZED PLATE WIDTH (x*)

Figure 5.6 : Effect of tube spacing on plate
temperature profile normal to the
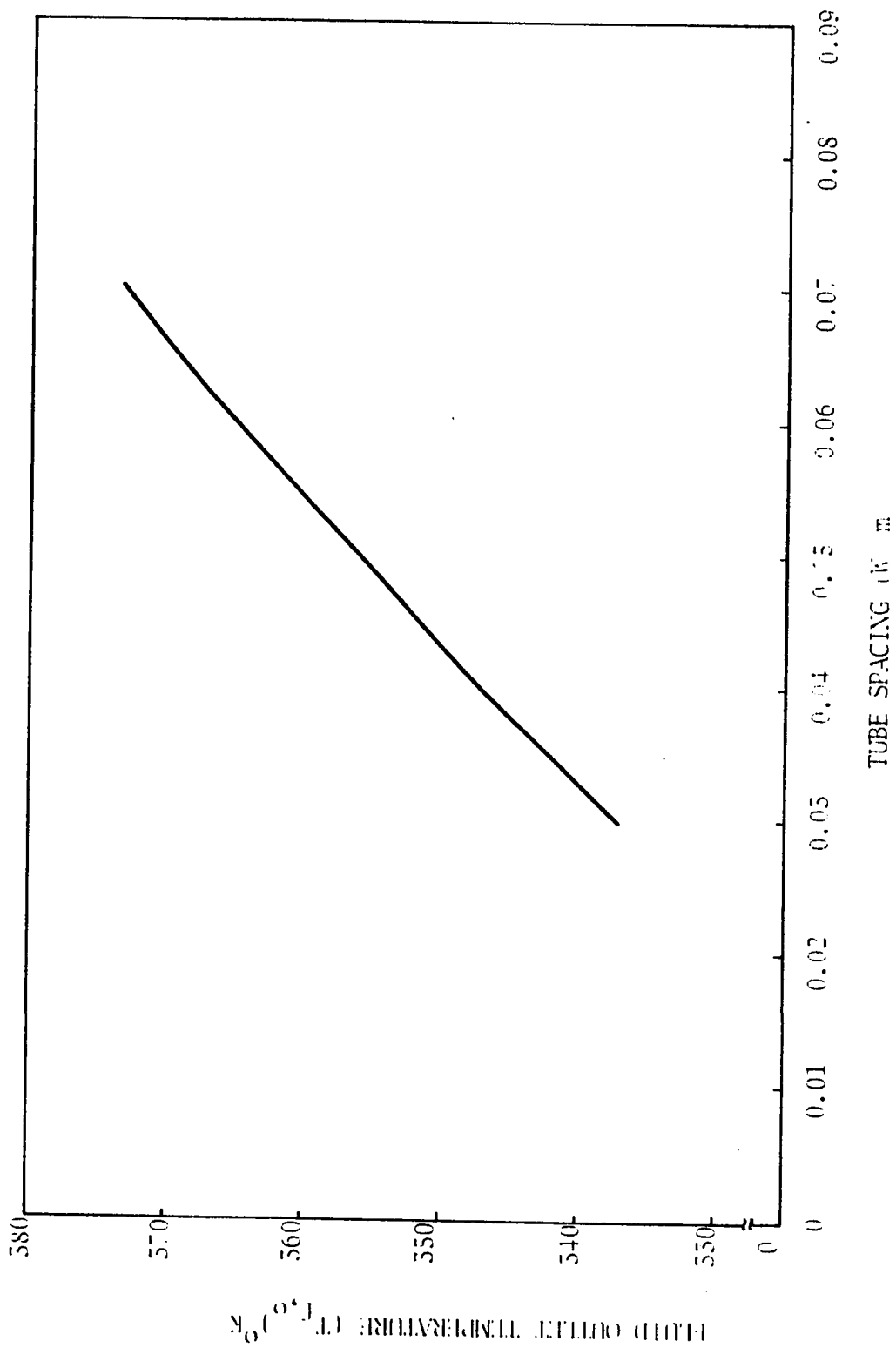tube for base-line conditions
and y* = 1.

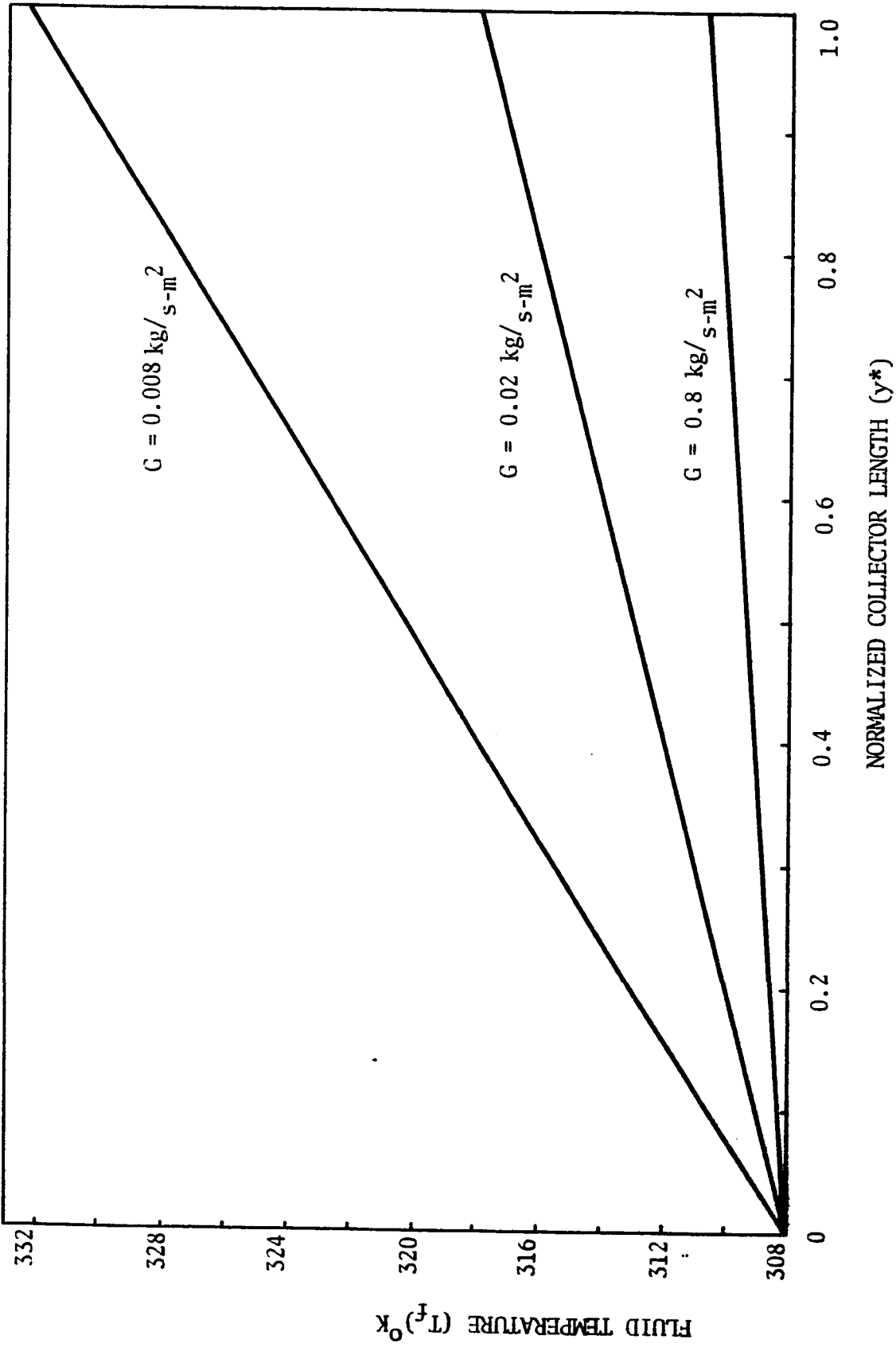Figure 5.7: Effect of tube spacing on fluid outlet temperature for base-line conditions.

Figure 5.8: Effect of mass flow rate on fluid temperature distribution along the tube for base-line conditions.

MASS FLOW RATE ($\dot{m}$), Kg/s

HWB MODEL

TWO-D MODEL

FLUID OUTLET TEMPERATURE ($T_{f,o}$), $^{\circ}K$

360

340

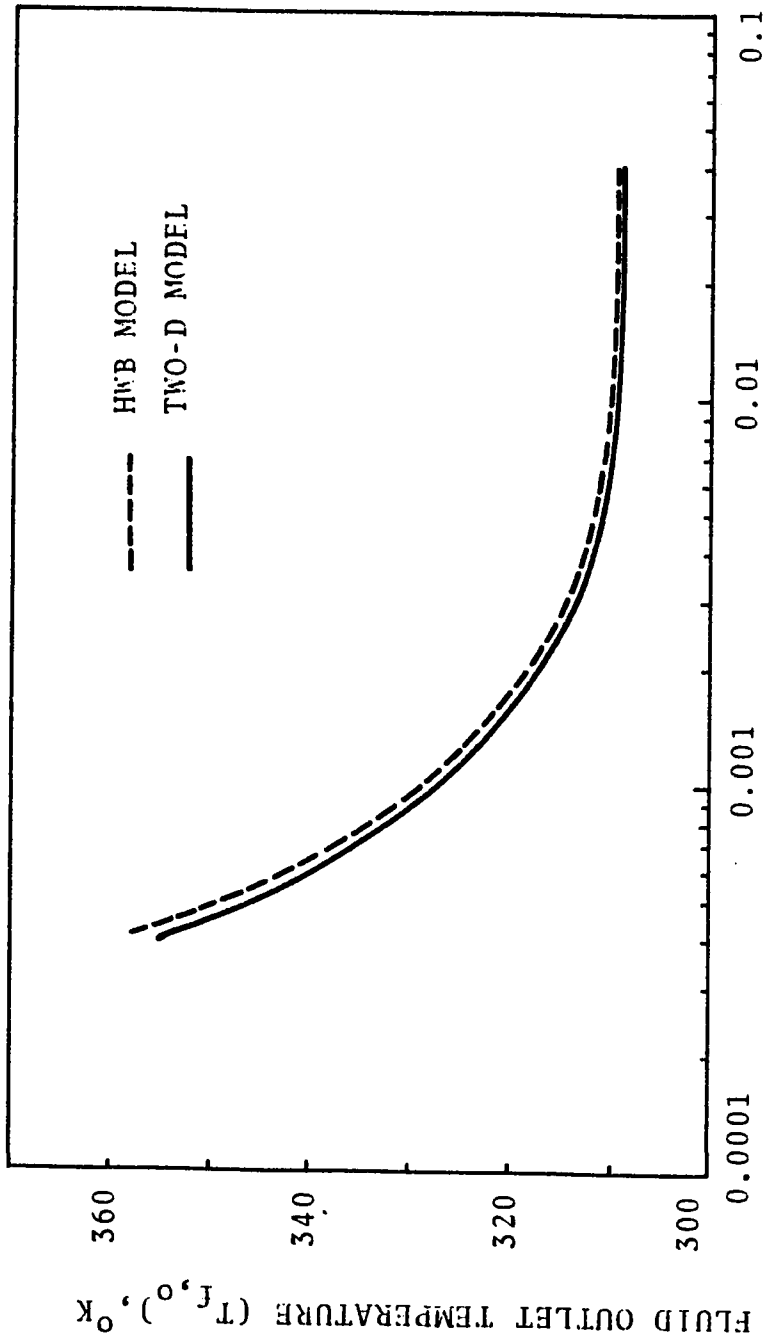320

300

0.0001

0.001

0.01

0.1

Figure 5.9:   Effect of mass flow rate on fluid outlet temperature for base-line conditions.

temperatures obtained from HWB model and continuous
line shows that obtained from two-dimensional model.
Observe that outlet fluid temperature obtained from
two-dimensional model is lower than that of HWB model.
This shows agreement with the results presented by
Phillips[10]. Axial conduction in the absorber plate
causes a flow of heat in the direction opposite to the
flow of fluid. This results in a reduction of the
fluid outlet temperature. Thus, fluid outlet temperatures
predicted by HWB model neglecting axial conduction are
higher. Note that the difference in fluid outlet temperatures
become very low at higher flow rates. The reason for this
trend can be seen by examining the isotherms in the fin,
Figures 5.3 and 5.4 as predicted from the two-dimensional
model. At high flow rate the isotherms are nearly parallel
to the water tube as assumed in the HWB model.

Effect of Fluid Inlet Temperature on Efficiency

Figure 5.10 illustrate the effect of increasing
the fluid inlet temperature on instantaneous collector
efficiency. Collector efficiency decreases as the fluid
inlet temperature is increased. Because high fluid inlet
temperatures results in high plate temperatures, giving
rise to increased losses and lower efficiencies. This
figure also presents a comparison of collector performance
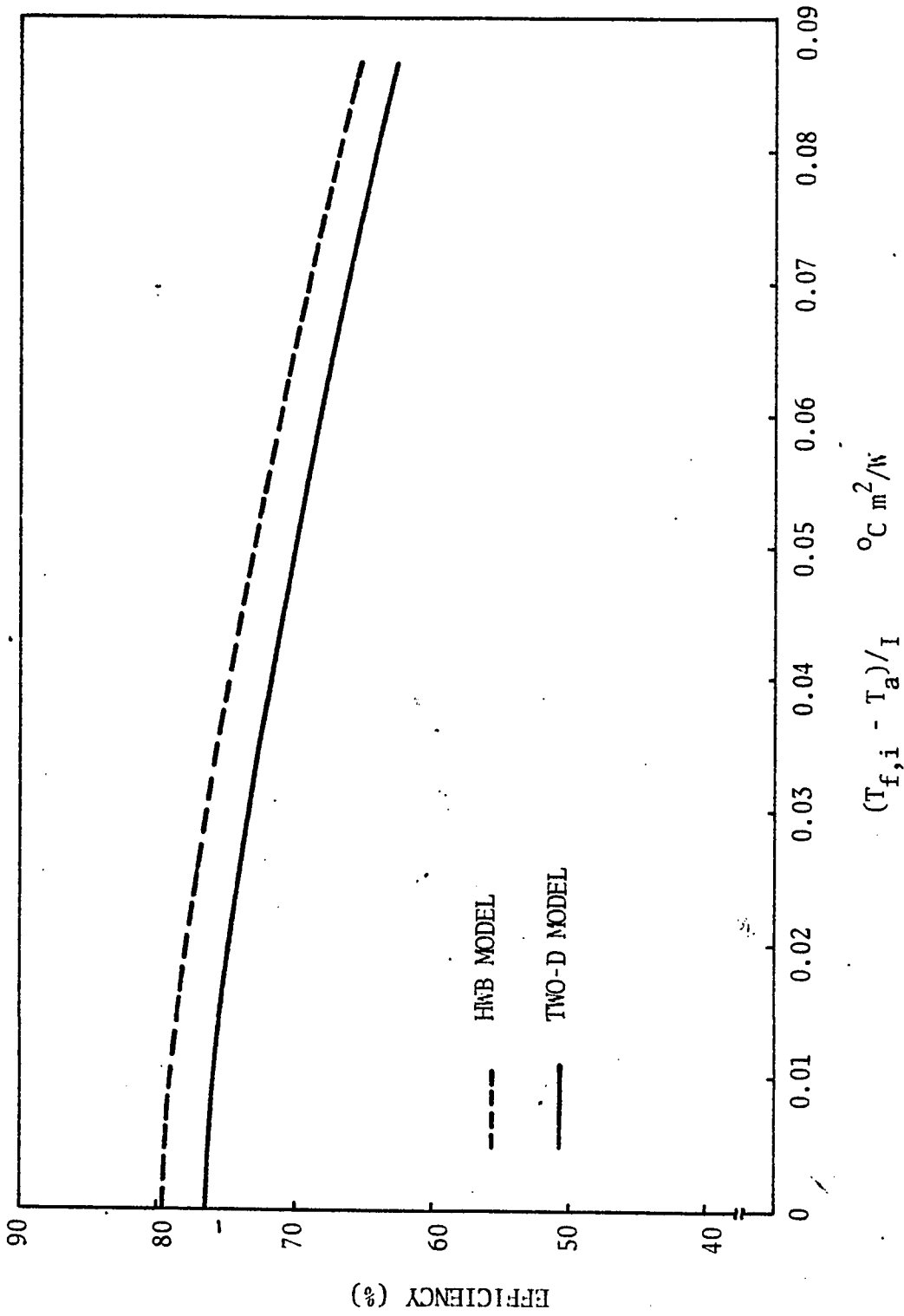between HWB model and two-dimensional performance model.

Figure 5.10: Effect of fluid inlet temperature on efficiency for base-line conditions.

It is observed that the discrepancy between the two curves is about 3 percent. This can be attributed to differences in the predicted fin and fluid temperature distributions discussed in the preceding section. Figure 5.11 shows variation of efficiency with average plate temperatures.

Effect of Flow Rate on Collector Efficiency

The effect of mass flow rate on efficiency is shown in Figure 5.12. The figure illustrates the strong influence of mass flow rate on collector efficiencies. As the mass flow rate is increased the collector performance increases and eventually approaches a maximum value asymtotically. Observe that the discrepancy between the two curves is more at low flow rate and gradually decreases as the flow rate becomes high as should be expected.

Effect of Tube Spacing on Efficiency

Figure 5.13 illustrate the effect of tube spacing on collector efficiency. Observe that decrease in tube spacing results in an increase in efficiency.

Effect of Collector Length on Efficiency

Figure 5.14 show the effect of collector length on efficiency. As collector length increases efficiency decreases.
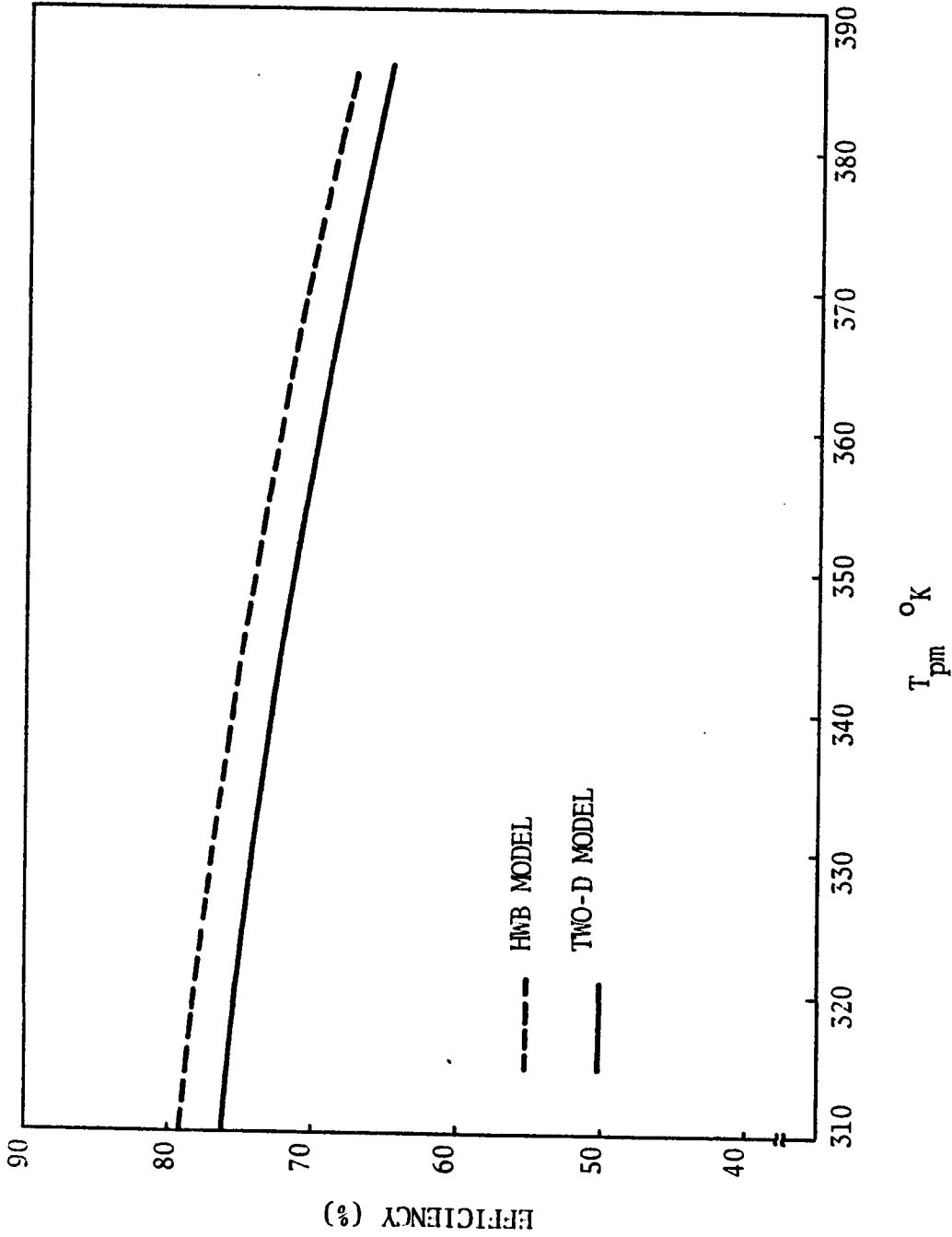
Figure 5.11: Efficiency versus average plate temperature for base-line conditions.
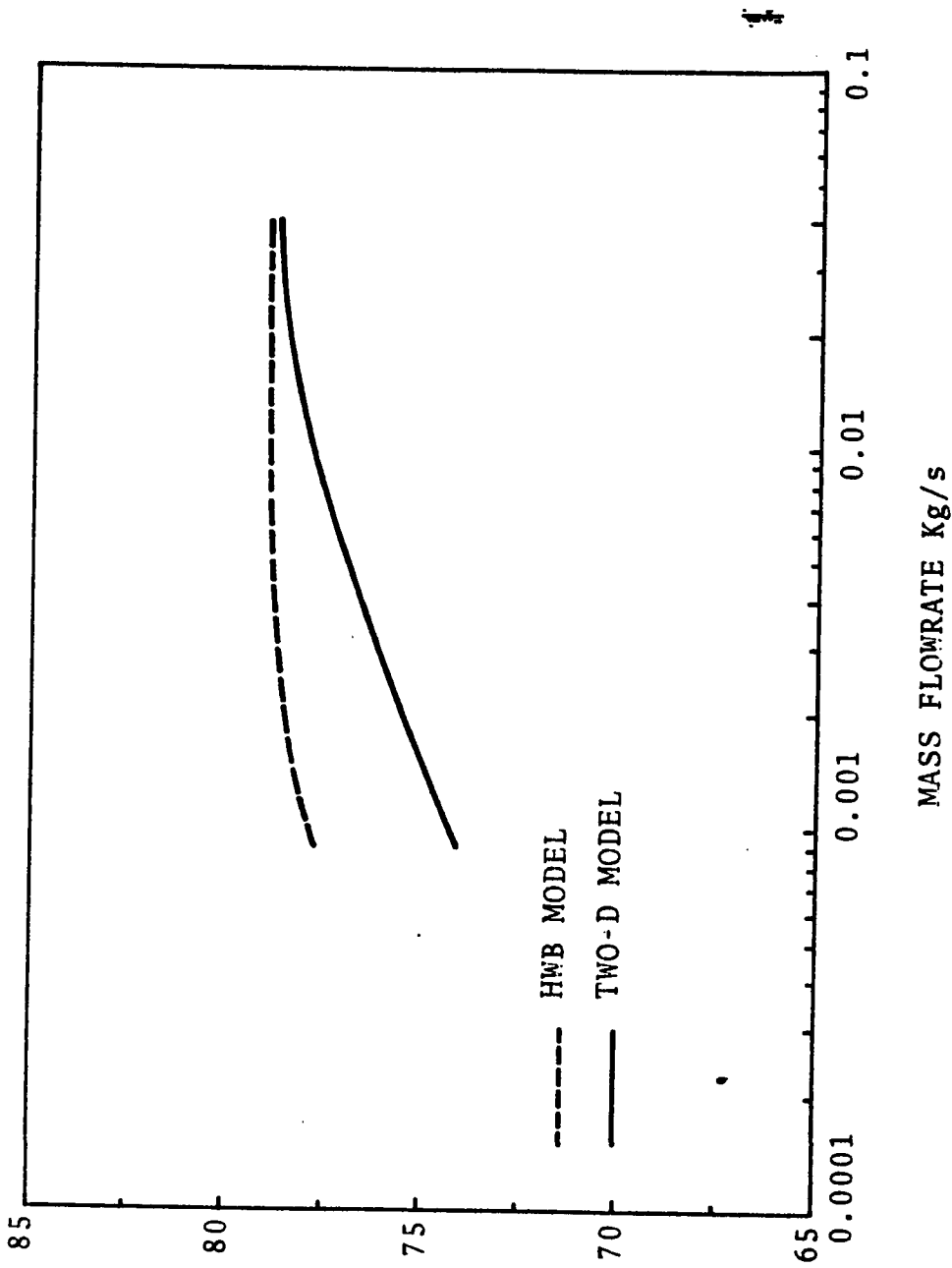
Figure 5.12 : Effect of mass flow rate on efficiency for base-line conditions.
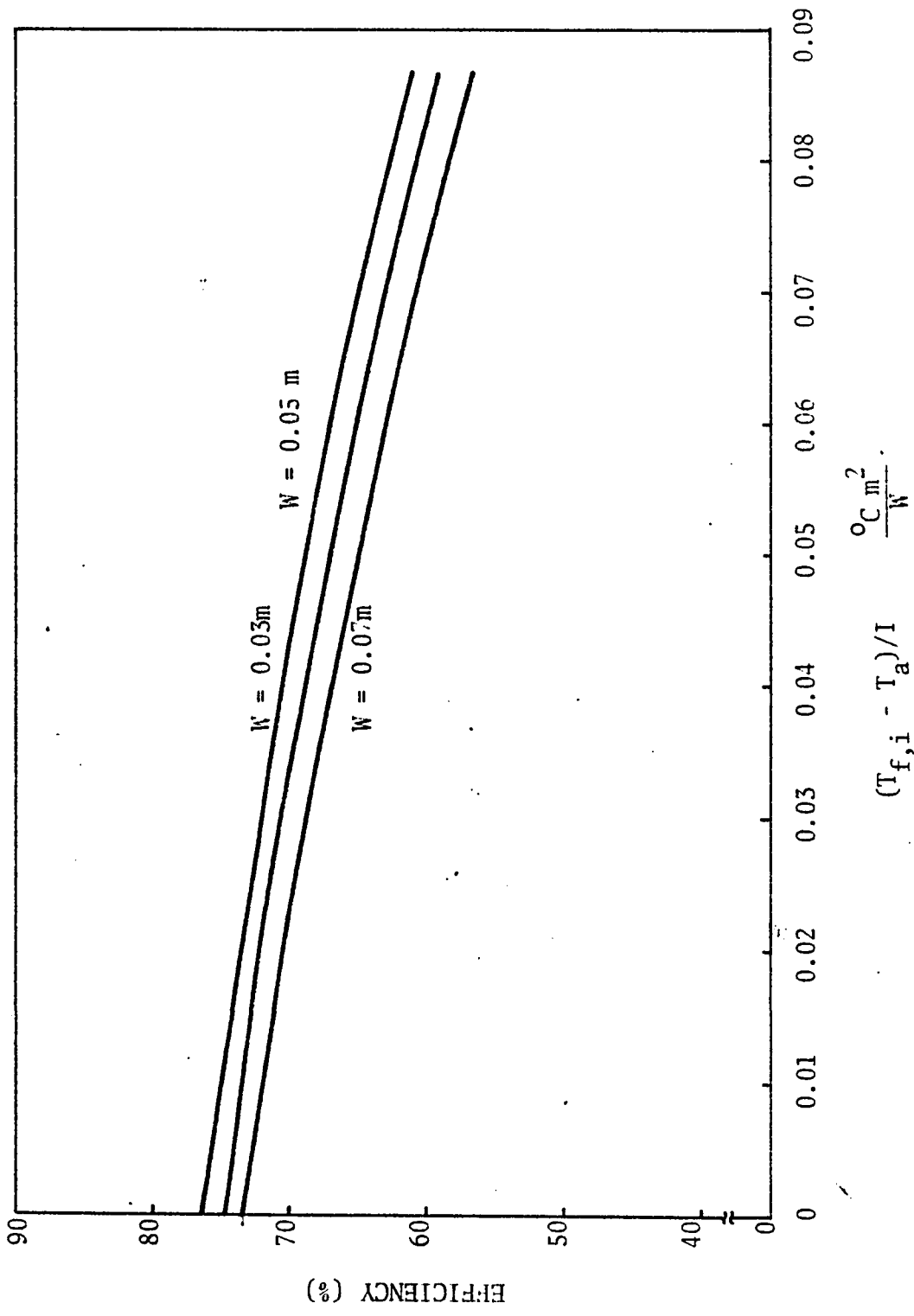
Figure 5.15: Effect of tube spacing on efficiency for base-line conditions
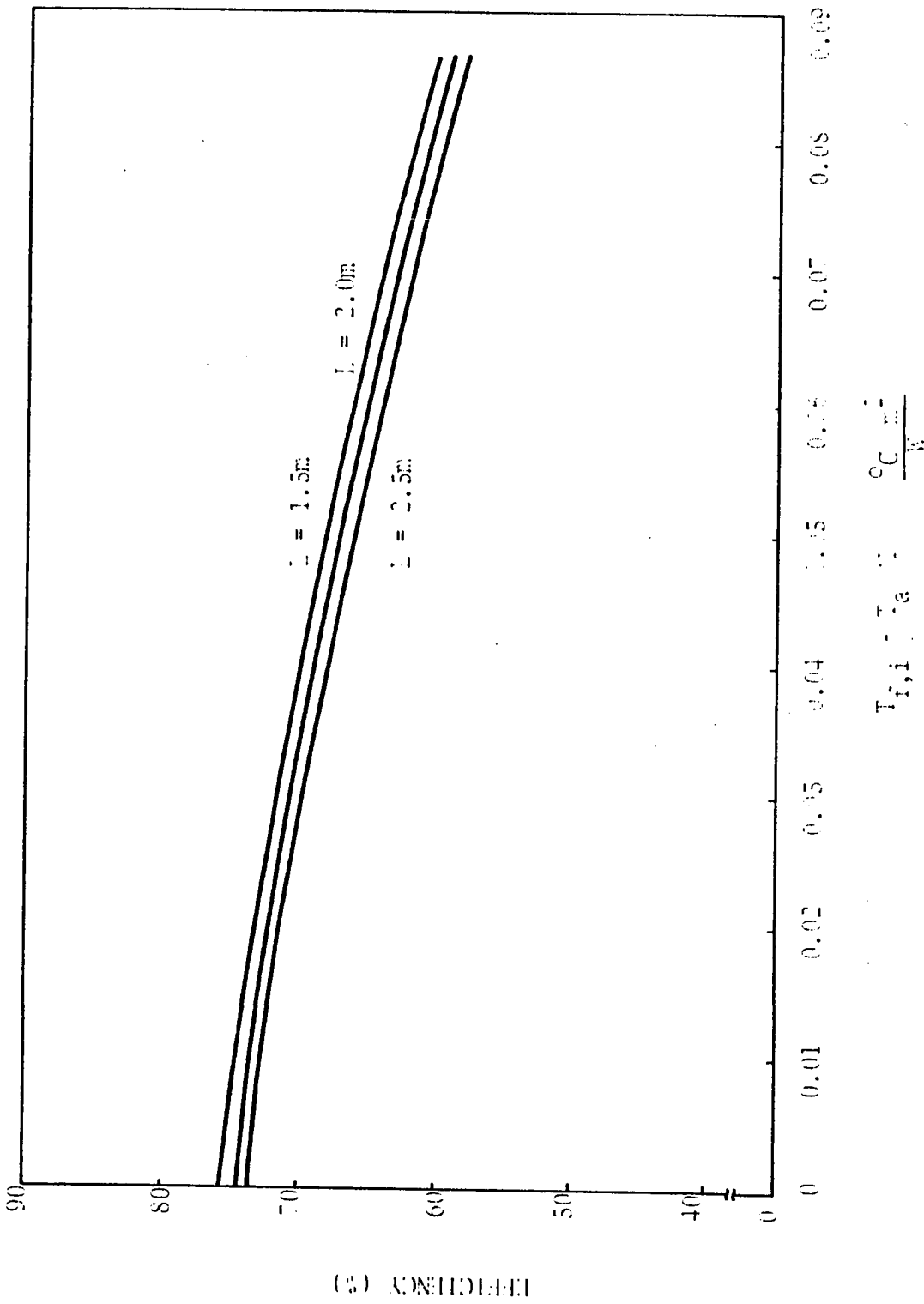
EFFICIENCY (%)

90
80
70
60
50
40
0

0   0.01   0.02   0.03   0.04   0.05   0.06   0.07   0.08   0.09

L = 1.5m

L = 2.0m

L = 2.5m

$$\frac{T_{f,i} - T_a}{I}$$

Figure 5.14: Effect of length on efficiency for base-line conditions

Effect of Plate Thickness on Efficiency

The effect of plate thickness on efficiency is shown in Figure 5.15. The curve in Figure 5.15 is obtained by changing plate thickness keeping thermal conductivity constant. Observe that plate thickness has very little effect on efficiency. So the plate thickness could be reduced considerably with no detrimental effect on performance, and an obvious decrease in material cost.

Conclusions and Recommendations

Evacuated tubular solar collector has been analysed considering two dimensional effects in the absorber plate. A two-dimensional model has been compared to the HWB model. Differences in the model of the heat transfer process in the absorber plate contribute to differences in predicted collector performance. Predicted temperature distributions are in agreement at high flow rate, and the isotherms structure indicates substantial heat flux parallel to the water tube at low flow rate. Correspondingly the discrepancy in performance between the two models is low at high flow rate and increases at lower flow rates.

A parameter study indicated that thinner plates would not sacrifice performance. Increase in tube spacing or length increases fluid outlet temperature and decreases
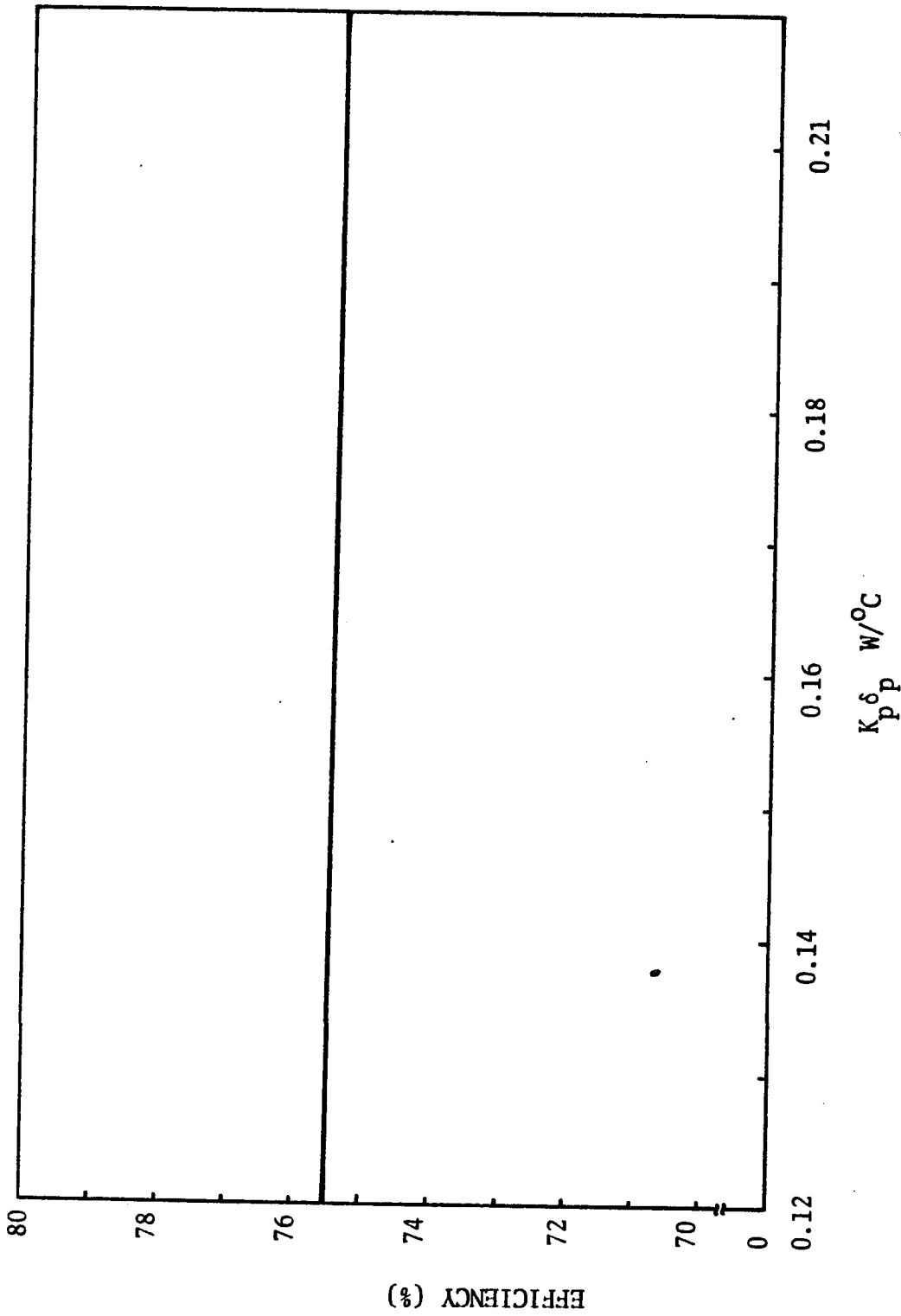
Figure 5.15: Effect of plate thickness on efficiency for base-line conditions.

efficiency, but it is more efficient to increase outlet fluid temperature by increasing length rather than water tube spacing.

The analysis made in the present study is specifically for an evacuated tube which uses flat plate as its absorbing surface. It can be modified for other designs of evacuated tube solar collectors. Using the two dimensional performance model, collector parameters can be optimized on the basis of least cost per unit of energy absorbed.

REFERENCES

1. Corning Glass Works, "Corning Tubular Evacuated Collectors", New York, (1975).

2. Klein, S.A., J.A. Duffie, and W.A. Beckman, "Transient Considerations of Flat Plate Solar Collectors", Trans ASME, J. Eng. Power 96A, pp 109-113 (1974).

3. Beekley, D.C. and Mather, G.R. Jr., "Analysis and Experimental Tests of a High Performance, Evacuated Tubular Collector", Owens Illinois, Inc. P.O. Box 1035, Toledo, Ohio, 43666.

4. Simon, F.F., "Solar Collector Performance Evaluation with the NASA-Lewis Solar Simulator - Results for an All-Glass-Evacuated Tubular Selectively Coated Collector with a Diffuse Reflector", NASA TMX-71695 (1975).

5. R. Bruno, et al, ISES-75, Extended Abstracts, pp 256-257 (1975).

6. Karaki, S. and Frick, D.M., "Performance of an Evacuated Tube Solar Collector", Colorado State University Solar Energy Applications Laboratory, (1976).

7. Hinotani, K., et al, "An Evacuated Glass Tube
    Solar Collector and Its Applications to a Solar
    Cooling, Heating and Hot Water Supply System
    for the Hospital in Kinki University", Solar
    Energy,Vol. 22, pp 535-545 (1979).

8. Felske, J.D., "Analysis of an Evacuated Cylindrical
    Solar Collector", Solar Energy, Vol. 22, pp 567-570
    (1979).

9. Duffie, J.A. and Beckman, W.A., "Solar Energy
    Thermal Processes, Wiley, New York, (1974).

10. Phillips, W.F., "The Effects of Axial Conduction
    on Collector Heat Removal Factor", Solar
    Energy,Vol. 23, pp 187-191 (1979).

11. Kirchhoff, R.H. and Billups, M., "A Two-Dimensional
    Heat Transfer Model of a Flat Plate Collector",
    ASME paper No. 76-WA/SOL-2 (1976).

12. Chiou, J.P., "Noniterative Solution of Heat
    Transfer Equation of Fluid Flow in Solar Collector",
    ASME Paper No. 79-WA/SOL-24 (1979).

13.   Hottel, H.C., and Woertz, B.B., "Performance of
       Flat-Plate Solar-Heat Collectors", Trans ASME
       64, 91 (1942).

14.   Hottel, H.C. and Whillier, A., "Evaulation of
       Flat-Plate Collector Performance", Transactions
       of the Conference on the Use of Solar Energy, 2,
       Part I, 74, University of Arizona Press, (1958).

15.   Bliss, R.W., "The Derivation of Several 'Plate
       Efficiency Factors' Useful in the Design of
       Flat-Plate Solar-Heat Collector", Solar Energy,
       3, 55, No. 4 (1959).

16.   Wilbur, P.J., Professor, Department of Mechanical
       Engineering, Colorado State University, Private
       Communication, May 22, 1980.

17.   Holman, P.J., Heat Transfer, McGraw Hill, New York,
       pp 142-148 and 158-169 (1963).

18.   Roberts, G.T., "Heat Loss Characteristics of an
       Evacuated Plate-In-Tube Collector", Solar Energy,
       Vol. 22, pp 137-140 (1979).

19.   Arpaci, V.S., Conduction Heat Transfer, Addison-
        Wesley Publishing Company, Reading, Massachusetts,
        pp 193-195 (1966).

20.   Finlayson, B.A., The Method of Weighted Residuals
        and Variational Principles, Academic Press, Inc.,
        New York, (1972).

A P P E N D I X "A"

COLLOCATION SCHEME

We select as many locations (y*'s) as there are undetermined parameters (C_n's) and then adjust the parameters until the residual vanishes at these locations. The presumption here is that the residual does not get very far away from zero in between the locations where it vanishes.

Equation (4.38) can be rearranged to form equation residual R(y*) as follows:

$$R(y_j^*) = [\sum_{n=o}^{k} \bar{C}_n \phi_n (y_j^*)] - \psi (y_j^*)$$

$$j = 1, 2, 3, \ldots K + 1$$

where $\psi (y^*) = g \ e^{-fy^*}$

In the present study, using collocation scheme with (K + 1) = 51 no significant changes in fluid outlet temperature were found. Hence in all the simulations the infinite series was truncated at 51 terms.